THE PLANT CELL

The Plant Cell, 2025, **37**, koaf200

https://doi.org/10.1093/plcell/koaf200
Advance access publication 16 August 2025
Research Article

Gibberellin transport affects lateral root growth through HY5 in response to far-red light

Kasper van Gelderen,[1,2,*] Kyra van der Velde,[1,3] Chia-kai Kang,[1] Jessy Hollander,[1] Alicia Koppenol,[1] Orfeas Petropoulos,[1,†] Putri Prasetyaningrum,[2,‡] Tuğba Akyüz,[1] Ronald Pierik[1,3,*]

[1]Plant-Environment Signaling, Department of Biology, Utrecht University, Padualaan 8, Utrecht 3584CH, The Netherlands
[2]Light Signaling and Cell Biology, Centre for Organismal Studies, Heidelberg University, Im Neuenheimer Feld 230, Heidelberg 69120, Germany
[3]Laboratory of Molecular Biology, Wageningen University and Research, Droevendaalsesteeg 1, Wageningen 6708PB, The Netherlands
*Author for correspondence: kasper.van.gelderen@cos.uni-heidelberg.de (K.v.G.), ronald.pierik@wur.nl (R.P.)
†Present address: RADICLE crops Wageningen.
‡Present address: Department of Molecular Plant Physiology, Faculty of Biology, University of Freiburg, Schänzlestrasse 1, 79104 Freiburg i. Br., Germany.
The authors responsible for distribution of materials integral to the findings presented in this article in accordance with the policy described in the Instructions for Authors (https://academic.oup.com/plcell/pages/General-Instructions) are: Ronald Pierik (ronald.pierik@wur.nl), and Kasper van Gelderen (kasper.van.gelderen@cos.uni-heidelberg.de).

Abstract

Plants compete for light by growing taller than their nearest competitors. This is part of the shade avoidance syndrome and is a response to an increase in far-red (FR) light reflected from neighboring leaves. The root responds to this shoot-sensed FR cue by reducing lateral root emergence. It is well established that the phytohormone gibberellic acid (GA) is involved in supplemental FR-induced shoot elongation. Although GA is transported from shoot to root, its role in regulating lateral root growth is unclear. Here, we chemically and genetically manipulated GA and showed that GA modulates the lateral root reduction induced by shoot-sensed FR enrichment in Arabidopsis (*Arabidopsis thaliana*). Using the FRET-based GA biosensor GPS1 (GIBBERELLIN PERCEPTION SENSOR 1), we observed detailed GA changes in the root upon shoot exposure to FR enrichment and upon GA application to the shoot. Supplying GA to the shoot mitigated the FR-enrichment-induced root phenotype, indicating a functional link between GA and changes in root development in response to shoot-sensed FR. The regulatory role of GA in root growth appears to be partially dependent on ELONGATED HYPOCOTYL 5 (HY5), a light-responsive transcription factor that regulates root growth. Shoot-to-root transported GA_4 led to increased HY5 protein levels in the lateral root primordia. HY5 then repressed auxin signaling, which inhibited lateral root growth. Our data reveal a gibberellin-dependent mechanism through which above-ground FR light signals modulate lateral root growth, whereby phytohormone and light signaling coordinate development across spatial scales.

Introduction

Light is an essential requirement for plant life and plants compete for light with other plants. Plants can detect competitors through reflection of far-red (FR) light from surrounding plants. This reflection increases the relative amount of FR, which is sensed through phytochromes (Franklin and Whitelam 2005). Phytochromes can be activated by red (R) light and inactivated by far red light. In a high R:FR ratio, phytochrome B (phyB) represses the PHYTOCHROME INTERACTING FACTORS (PIFS), by binding and targeting them for 26S proteasome degradation (Ni et al. 2013; Shin et al. 2016). In a low R:FR ratio, indicative of neighbor proximity, phyB is inactivated and PIFs can activate shade avoidance responses of the shoot (elongation growth, early flowering Ballaré and Pierik 2017). Low R:FR detected by the shoot can also lead to a reduction in lateral root density and main root length in Arabidopsis and this is regulated via the bZIP transcription factor ELONGATED HYPOCOTYL 5 (HY5) (van Gelderen et al. 2018).

Gibberellins (GA) are a class of growth promoting hormones that are also involved in the developmental responses of the shoot to FR light (Hisamatsu et al. 2005; Djakovic-Petrovic et al. 2007; Bou-Torrent et al. 2014; Crocco et al. 2015). Low R:FR treatment enhances GA biosynthesis, while at the same time increasing the responsiveness of the plant to it (Reed et al. 1996; Hisamatsu et al. 2005). Gibberellin sensing occurs via the interaction between the GA sensor GIBBERELLIN INSENSITIVE DWARF1 (GID1) and DELLA repressor proteins (Schwechheimer 2012). GA promotes GID1 binding to DELLAs which leads to the proteasomal degradation of the latter. DELLAs bind and repress the BRASSINAZOLE RESISTANT—AUXIN RESPONSE FACTOR—PIF (BAP) transcription factors module. These transcription factors together regulate cell expansion and thus also light-mediated cell elongation (Oh et al. 2014). The DELLA proteins form a brake on this BAP module, allowing GA-mediated degradation of DELLAs to release that brake and initiate shade avoidance responses (Davière and Achard 2016).

The shade avoidance response of the plant occurs throughout the entire plant body, but the sensing is confined to the leaves and stem of the plant, thus requiring a co-ordination between organs by signaling molecules (Küpers et al. 2018). Especially the response of the root system requires a long-distance communication between shoot and root, since the root does not sense the light when growing in dark soil. HY5 is involved in the root response to FR light detected by the shoot (van Gelderen et al. 2018) and can be transported over longer distances, affecting nitrate uptake, phosphate and iron uptake (Sakuraba et al. 2018; Guo et al. 2021), and

Received April 04, 2025. Accepted July 3, 2025.

root growth (Chen et al. 2016; van Gelderen et al. 2021). In the root, HY5 acts by repressing auxin transport and signaling (Cluis et al. 2004; Sibout et al. 2006; van Gelderen et al. 2018), and it is specifically increased at the lateral root primordia when the shoot detects a low R:FR ratio (van Gelderen et al. 2018).

Gibberellins regulate shoot and root growth processes (Hedden and Sponsel 2015). For the root, the concentration of GA needed to sustain growth is lower than the shoot (Tanimoto 1994), and an overly high concentration can even slow down root growth (Inada and Shimmen 2000). GA, through repressive effects on DELLAs, regulates the size of the root apical meristem (RAM) and root cell size, and GA acts in, and is synthesized in, the endodermis layer of the root tip (Ubeda-Tomás et al. 2008, 2009; Barker et al. 2021). Crucially, GA can also be transported from shoot to root (Binenbaum et al. 2018). Bioactive gibberellin, such as GA_3 and GA_4, can be traced from the shoot to the root tip through the phloem, where it unloads into the endodermis (Shani et al. 2013; Tal et al. 2016). Furthermore, it was shown that functional GA biosynthesis in the shoot is necessary to drive root growth and that even a precursor of bioactive GA, GA_{12}, can be transported from shoot to root, where it is converted into bioactive GA (Regnault et al. 2015).

Here, we investigate how GA regulates root growth plasticity in response to aboveground FR cues of neighbor proximity. We show that shoot-to-root transport of GA can modulate the root response to supplemental shoot FR, and identify local GA changes using the GPS1 (GIBBERELLIN PERCEPTION SENSOR 1) GA biosensor (Rizza et al. 2017). Furthermore, we identify a role for HY5 in regulating the GA response and show that GA can affect HY5 abundance in the root.

Results

GA and paclobutrazol application modify effect of supplemental FR on lateral root development

In order to investigate whether GA plays a role in the response of the root system to supplemental FR light we performed dose–response experiments. We illuminated the shoot with supplemental FR light (WL + FR) to lower the R:FR ratio and used D-root plates (Silva-Navas et al. 2015) to avoid direct illumination of the root system (van Gelderen et al. 2018, 2021). Seeds were germinated on ½ MS control media, transferred after 1 d to either control or GA-containing ½ MS media (Supplementary Fig. S1A), and transferred after 4 d to new plates (van Gelderen et al. 2018). We used the GA_4 form of Gibberellic acid, since it is a more prevalent bioactive form in Arabidopsis than the often used GA_3 (Prasetyaningrum et al. 2020), with a good affinity to the gibberellin sensor GID1 (Yoshida et al. 2018). However, we compared its effect against that of GA_3, which confirmed that GA_4 is a more potent gibberellin than GA_3 (Supplementary Fig. S1). Thus, we continued the use of GA_4 in subsequent experiments. GA_4 application led to increased hypocotyl growth in both light conditions, with the relative FR response decreasing slightly in GA_4 treatment (Fig. 1A). Up to 10^2 nM GA_4, main root growth was unaffected, however at 10^3 nM there was an increase in main root length (Fig. 1D). Interestingly, 10^4 nM of GA_4 led to a strong decrease in main root length, coupled to an increase in root hair formation, and agravitropic root growth (Fig. 1, D and E). Lateral root density in control treatment decreased due to WL + FR, but GA_4 application at 10^0 to 10^2 nM negated this effect (Fig. 1, B and E) (except at 10^3 nM GA_4) of GA_4, while at 10^4 nM very few lateral roots emerged at all (Fig. 1, B and E). WL + FR decreased the lateral root zone length, also called the branching zone, which is the length of the main root between the first and last emerged initial (Fig. 1C). GA_4 application removed the negative effect of WL + FR on lateral root zone length, varying with the concentration of GA_4 (Fig. 1C).

Paclobutrazol (PAC) is a drug that inhibits the conversion of *ent*-Kaurene into *ent*-Kaurenoic acid, a crucial first step in gibberellin biosynthesis that is performed by the GA1 enzyme (Rademacher 2000). Genetically knocking out GA1 leads to a dramatic loss of GA production, however by dosing the amount of PAC one can gradually inhibit biosynthesis of GA. We grew Col-0 seedlings in a dose-response experiment similar to the one presented in Fig. 1, however now we used 0, 10^2, 10^3, and 10^4 nM of PAC. PAC treatment led to a decrease in WL + FR-induced hypocotyl elongation that was completely removed at 10^4 nM PAC (Fig. 2A). 10^2 nM PAC reduced the lateral root density and prevented further reduction induced by WL + FR (Fig. 2B). Lateral root density was further reduced by 10^3 nM PAC, however, at 10^4 nM it rose sharply (Fig. 2B); This strong increase can be attributed to a dramatic decrease in main root length (Fig. 2, C and D), thus concentrating the lateral roots on a shorter main root. Interestingly, while the main root was smaller than 1 cm on average in this very high PAC concentration, still some lateral roots could emerge (Fig. 2D). Additionally, we tested the *ga1-3* mutant, which is defective in the GA1 biosynthesis enzyme, and found that the WL + FR response was lost in this mutant (Supplementary Fig. S1F). Both the addition of GA_4 and PAC to the growth medium leads to the loss of the effects brought on by the WL + FR treatment. Therefore, we conclude that gibberellins can modulate the shoot and root response to shoot-applied FR light.

Supplemental FR light to the shoot increases GA in the root

Since GA_4 addition leads to the loss of WL + FR effects on lateral root development, we chose to investigate whether WL + FR would lead to changes in the levels of GA in the root system. To do this we used the GPS1 Förster resonance energy transfer (FRET) sensor, that is able to detect relative levels of active Gibberellins by measuring the ratio in YFP to CFP signal that are fused to a truncated GID1 and DELLA (GAI) (Rizza et al. 2017, 2021) (Fig. 3A). Four-d-old seedlings were transferred to control or 10^2 nM GA_4 plates and after 2 d were fixed via the ClearSee method (Ursache et al. 2018). First, we checked if the GPS1 sensor was responsive in the root to GA_4 addition to the plate medium. Both in the RAM and the lateral root primordium did we see a pronounced increase in the YFP/CFP ratio when 10^2 nM of GA_4 was applied (Fig. 3B), which corresponds to an increase in the bioactive GA level. The non-responsive control sensor GPS1-NR did not react to external GA application (Fig. 3C). A treatment of WL + FR during 2 d led to an increase in the GPS1 ratio in the elongation zone of the root meristem (Fig. 3, D, G, and H), which is interesting since the elongation zone has been identified as a region where shoot-borne GA_4 can be transported to (Shani et al. 2013). In the lateral root primordia we also observed an increase in the YFP/CFP GPS1 ratio, across all stages (Fig. 3E), and mainly in Stages 4 and 5 (Fig. 3, F, I, and J). These GPS1 data show that WL + FR, as detected by the shoot, leads to an increase in GA levels in root tissues, particularly around the elongation zone and in the lateral root primordia, which are regions important for main root growth and lateral root development respectively.

GA_4 application to the shoot reduces root growth and removes WL + FR effect on root development

Several reports have alluded to potential roles for GA transport from the shoot to the root in affecting root development

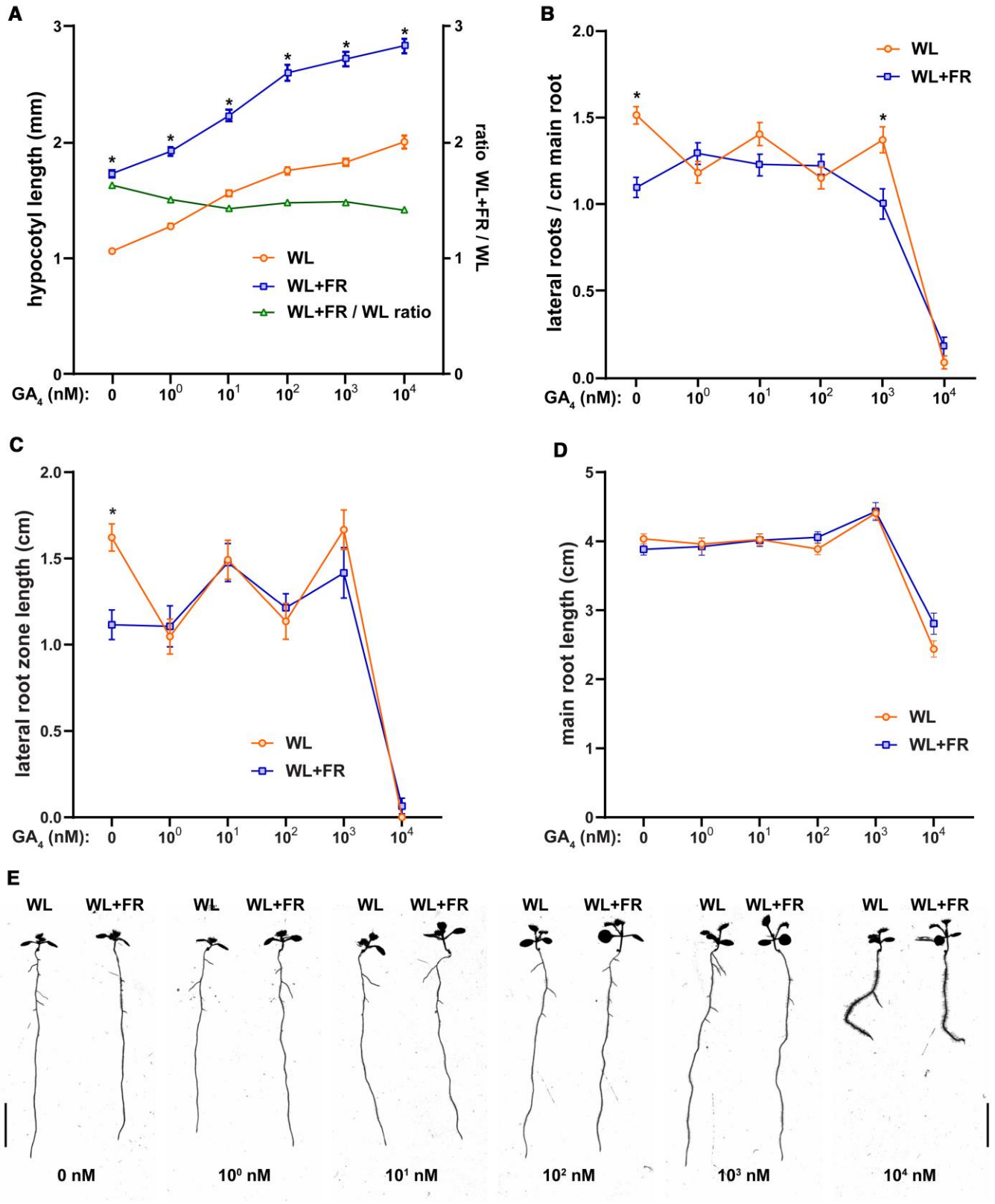

Figure 1. GA_4 application modifies the response of the root to supplemental FR light. Seedlings were grown for 9 d according to the schedule on Supplementary Fig. S1A. Scans of 9-d-old seedlings were analyzed on **A)** hypocotyl length, with the ratio between WL + FR/WL displayed on the right axis and in green; **B)** main root length; **C)** lateral root density; **D)** lateral root zone length. **E)** Representative seedling images of the experiment, scale bar = 1 cm. (All graphs) Means were statistically significant based on a 2-way ANOVA; letters denote significant difference between treatments based on a post hoc Tukey test ($P < 0.05$). For 0 to 10^3 nM $n \geq 30$, for 10^4 $n = 20$; error bars show the SEM.

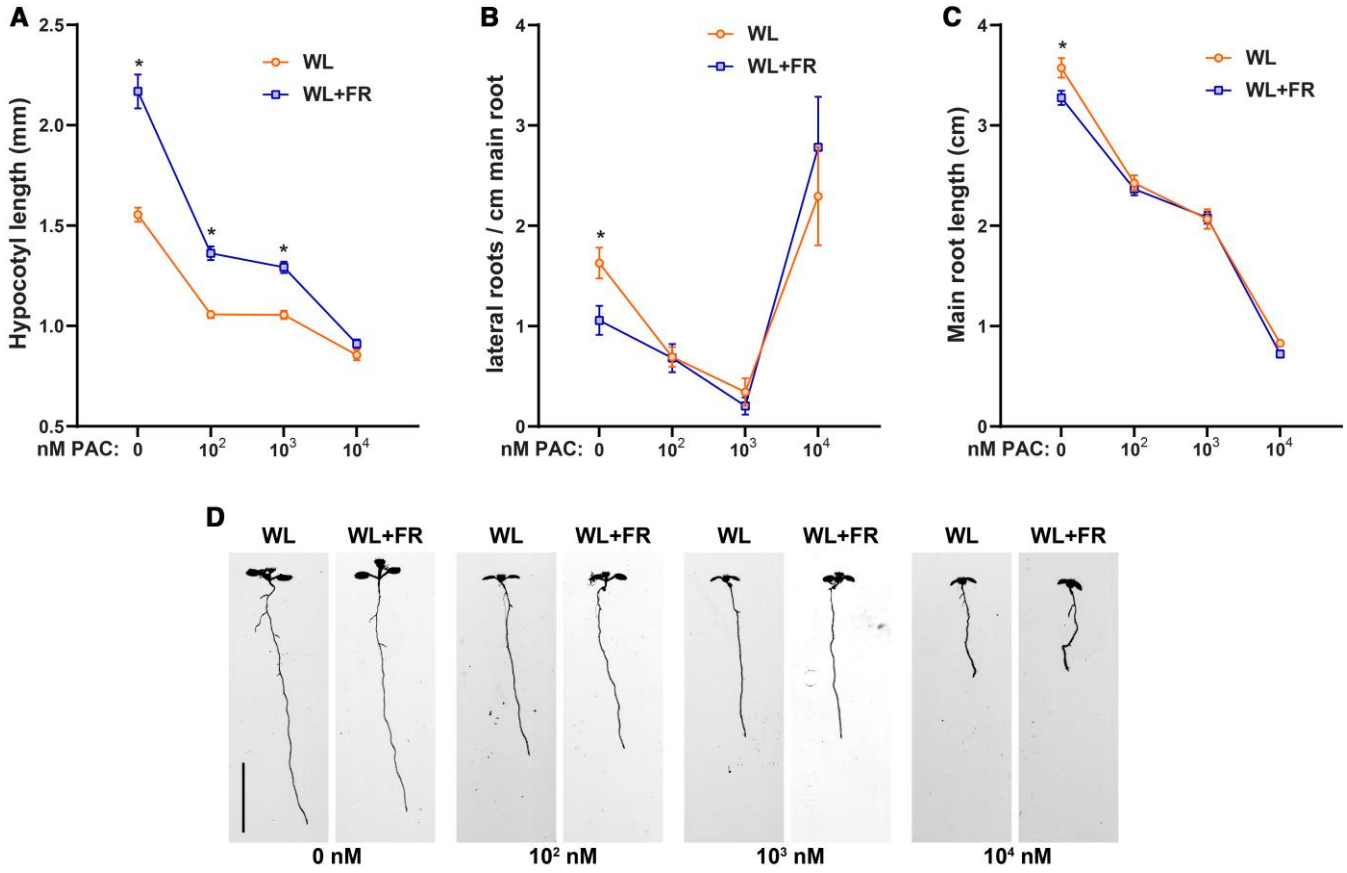

Figure 2. PAC treatment reduces root growth and removes the effects of WL + FR on hypocotyl and root development. Seedlings were grown for 9 d according to the schedule on Supplementary Fig. S1A. Scans of 9-d-old seedlings were analyzed on **A)** hypocotyl length; **B)** lateral root density; **C)** main root length; **D)** representative seedling images of the experiment, scale bar = 1 cm. (All graphs) Means were statistically significant based on a 2-way ANOVA; letters denote significant difference between treatments based on a post hoc Tukey test ($P < 0.05$, $n = 20$); error bars show the SEM.

(Shani et al. 2013; Regnault et al. 2015; Binenbaum et al. 2018). We detected an increase in GA in WL + FR via the GPS1 sensor. Since in our setup, WL + FR is only detected by the shoot, these findings could suggest that WL + FR leads to increased transport of GA from shoot to root. In order to test this notion, we wanted to see if shoot-applied GA_4 can lead to root developmental changes. Therefore, we designed square petri-plates where we could separate a shoot and root compartment by a physical barrier of 3 mm height, so that different layers of agar could be poured but not diffuse into each other (Supplementary Fig. S2). We grew seedlings for 4 d on normal square plates on ½ MS medium without GA_4 and then transferred them to the 2-compartment plates containing control (EtOH 1:10000) or 10^2 nM GA_4 medium in the respective compartments (Fig. 4A). We took extra care to position the seedlings such that the hypocotyl and cotyledons, but not the root touched the medium in the upper compartment and we carefully placed the root over the plastic barrier, so that it touched medium in the bottom compartment (Supplementary Fig. S2C). We used a full factorial combination of GA and control (EtOH) in the top or bottom compartment (EtOH/EtOH, GA_4/EtOH, EtOH/GA_4, GA_4/GA_4). After 5 d of growth on the compartment plates we scanned and analyzed hypocotyl length and root traits (Fig. 4B). Hypocotyl length was increased only on the plates which contained GA_4 medium in the top compartment (GA_4/EtOH and GA_4/GA_4) (Fig. 4C). However, main root length was negatively affected by GA_4, irrespective of it being in the top or bottom compartment or both (Fig. 4D). Similarly, lateral root density and lateral root zone length were negatively affected in the same manner if GA_4 was given directly to the bottom compartment or only to the shoot (GA_4/EtOH, EtOH/GA_4) and GA_4/GA_4) (Fig. 4, E and F). This shows that supplying the root with GA_4 does not lead to hypocotyl elongation, however, when the shoot is in contact with GA_4 medium the effect on the root system is the same as when the root itself is in GA_4 medium. This indicates that shoot-to-root transport of GA_4 may play a role in changing main and lateral root development, although an intermediate mobile messenger cannot be ruled out yet.

Next, we tested whether application of GA_4 to the top compartment would remove the effect of WL + FR on lateral root growth, similar to application on the whole plate (Fig. 1B). After the 4-d-old seedlings were transferred to either an EtOH/EtOH or a GA_4/EtOH plate, these plates received either WL or WL + FR (Fig. 4G). Hypocotyl length after 6 additional days of growth was increased on GA_4/EtOH plates and also by WL + FR, in a manner very similar to GA_4 application on the whole plate (Figs. 4H and 1A). WL + FR led to a reduction in lateral root density on EtOH/EtOH plates, as did GA_4/EtOH, WL + FR did not affect lateral root density any more on GA_4/EtOH plates (Fig. 4I). In all these experiments of Fig. 4, 10^2 nM GA_4 application led to a reduction in main and lateral root growth, contrary to the results in Fig. 1. This is possibly due to the different timing of GA_4 exposure: 4 d after germination in Fig. 4, versus 1 d after germination in Fig. 1.

Overall, the results on these compartmentalized plates indicate that shoot-borne GA_4 can affect lateral root development

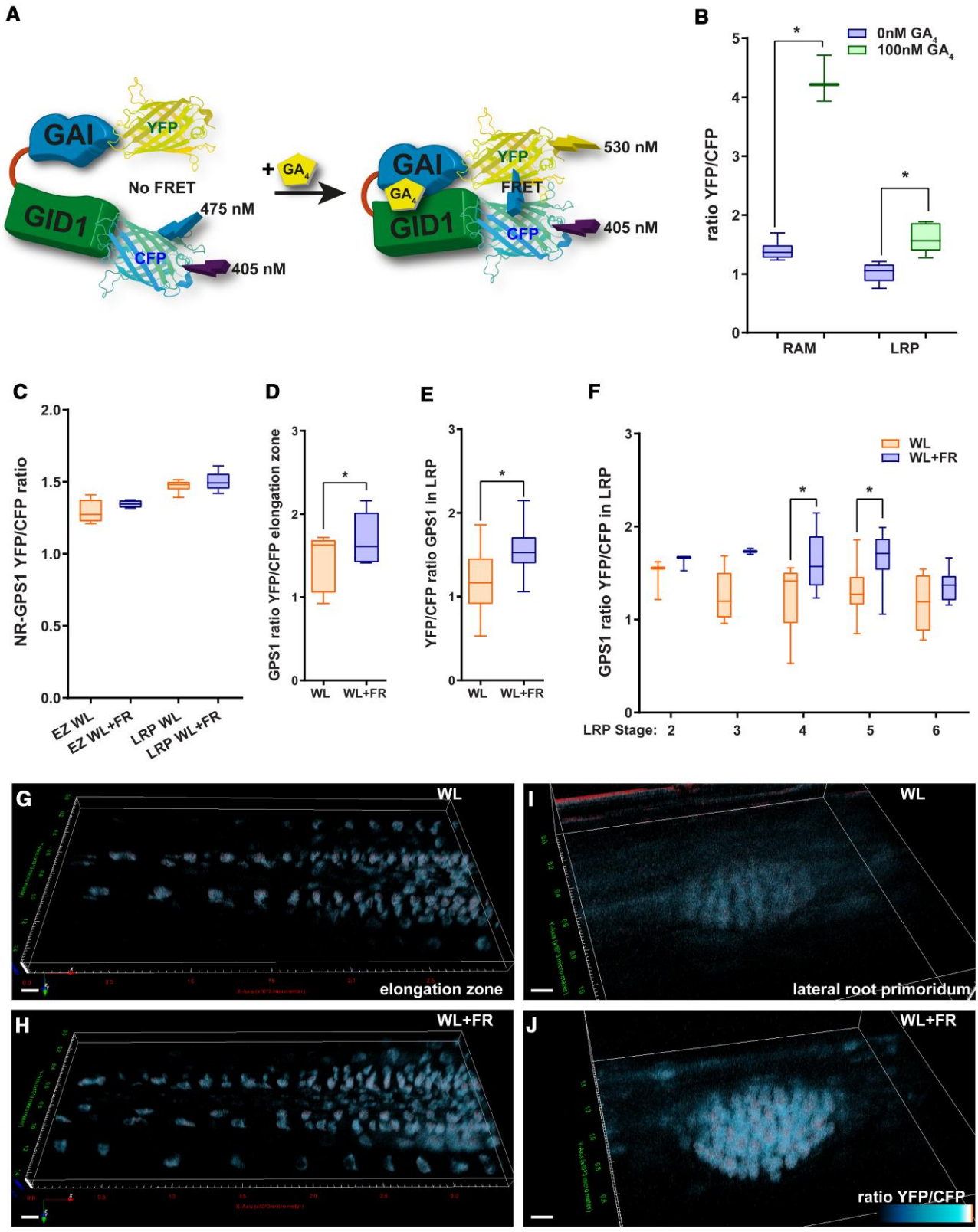

Figure 3. WL + FR leads to increased GA as detected via the GPS1 sensor. Confocal microscopy experiment with quantifications **B** to **F)** and representative images **G** to **J)**. **A)** Cartoon explaining the principle behind detecting bioactive GA with GPS1 (based on Rizza et al. 2017). **B)** Ratio between YFP and CFP emission of GPS1 in 6-d-old seedlings treated with mock or GA_4 for 2 d and similar data for the nonresponsive (NR) variant of GPS1 **C)** ($n = 9$). **D** to **F)** GPS1 ratio in 6-d-old seedlings treated with WL or WL + FR for 5 d; (All graphs) *significant difference based on student's *t*-test **D** and **E)** and 1-way ANOVA **F)** ($P < 0.05$, $n = 19$); whiskers show the distribution. **G** to **J)** representative YFP/CFP ratiometric 3D-rendered images of experiments in **D** to -**F)**; scale bar = 10 μm.

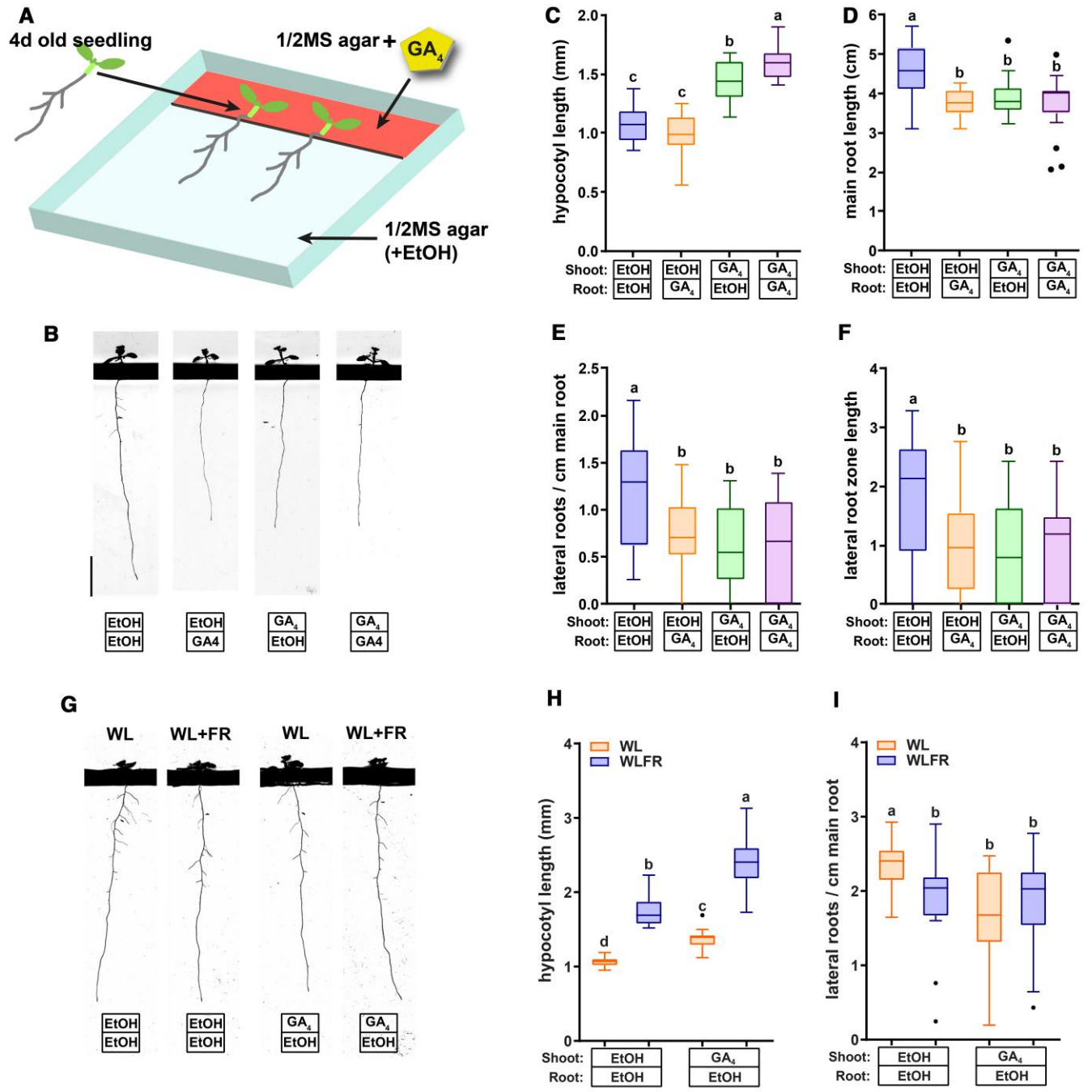

Figure 4. Compartmentalized plates show that shoot applied 10^2 nM GA_4 affects (lateral) root growth similarly to 10^2 nM GA_4 applied directly at the root. **A)** Overview of the experimental procedure. A barrier of 3 mm high is present on the plate that physically isolates 2 agar layers. The top layer is 3 cm long, while the bottom one is 9 cm. Seedlings are first grown on normal ½ MS for 4 d, and then they are transferred so that the start of root is carefully positioned over the barrier. **B** to **F)** Nine-d-old Col-0 wild-type seedlings grown in WL on compartmentalized plates with different media combinations. **B)** representative seedlings, black bar is the physical barrier on the plate, scale bar = 1 cm; **C)** hypocotyl length, **D)** main root length; **E)** lateral root density; **F)** lateral root zone length. **G** to **I)** Ten-d-old Col-0 wild-type seedlings grown in WL or WL + FR on medium with or without GA_4 in the top compartment. **G)** Representative seedlings, scale bar = 1 cm; **H)** hypocotyl length; **I)** lateral root density. (All graphs) Means were statistically significant based on a 2-way ANOVA; letters denote significant difference between treatments based on a post hoc Tukey test ($P < 0.05$, **C** to **F**: $n \geq 15$, **H** and **I**: $n \geq 20$); whiskers show the distribution.

and can modulate the response to shoot perceived WL + FR. A previous report indicates that GA_{12} is a shoot-to-root mobile gibberellin (Regnault et al. 2015). We, therefore, verified whether GA_{12} application on the shoot would lead to comparable effects on lateral root growth to GA_4 application and whether GA_{12} can rescue the WL + FR effect similarly to GA_4. We again used a system where we separated the top and bottom compartment of the agar plate (Supplementary Fig. S2, E and F), and applied 20 nM GA_{12} to the shoot. GA_{12} application had a small but significant effect on hypocotyl length in WL + FR (Fig. 5A). However, neither lateral root density, nor the effect of WL + FR were significantly altered by GA_{12} in wild type (Fig. 5, B to F). GA_{12} is a precursor to bioactive GA, and in

Arabidopsis is not considered biologically active. It is produced from ent-kaurenoic acid by the ent-kaurenoic acid oxidase (KAO) enzymes (Regnault et al. 2014). We also tested the *kao1-2 kao2-3* double mutant for responsiveness to WL + FR and GA_{12}. *kao 1 kao2* double mutants are severely hampered in GA_{12} production (Regnault et al. 2014, 2015). GA_{12} application could restore part of the low R:FR-induced hypocotyl elongation in the *kao* double mutant (Fig. 5A). Interestingly, the *kao1-2 kao2-3* double mutant still had a reduction in lateral root development due to WL + FR and strikingly, GA_{12} application to the shoot promoted lateral root zone length and density of this double mutant specifically under WL + FR-induced condition (Fig. 5, C to F). This result shows that GA_{12} could play a role in transducing the WL + FR signal and phenotype, but equally likely, it could be GA_4 produced from GA_{12}. Thus these results do not answer whether GA_{12} or GA_4 is the dominant factor in transducing the FR signal from the shoot, especially since a *kao1 kao2* mutant was found to still have small amounts of GA_4 in its tissues (Regnault et al. 2014). Therefore, we maintain the hypothesis that both GA forms are likely to be transported from shoot to root. After showing the particular efficacy of shoot-applied GA_4 in regulating lateral root development, we next wanted to know how application of GA_4 on the shoot would affect the levels of bioactive GA as measured by the GPS1 sensor.

GA_4 applied on shoot leads to significant changes in bioactive GA in the root

In order to assess relative GA levels with the GPS1 sensor, we performed a similar experiment as shown in Fig. 4; however, this time we used GPS1 seedlings that were fixed and cleared with ClearSee 2 d after transfer to preserve them for confocal microscopy imaging (Fig. 6). We observed that GA_4 application to the shoot compartment led to an increase in in the YFP/CFP GPS1 ratio in the hypocotyl (Fig. 6, A, E, and F). Then, moving down toward the root tip we observed a significant increase in GPS1 ratio in the lateral root primordium due to GA_4 application to the shoot (Fig. 6, B, G, and H). Importantly the GPS1 ratio was only increased in the inner layers of the root that are enclosed by the Casparian strip of the endodermis: the stele, pericycle, and endodermis, while the cortex and epidermis layers did not show an increase of the GPS1 ratio (Fig. 6, G to J). In comparison, when GA_4 was applied to the whole plate, the GPS1 ratio increased also in the cortex and epidermis (Supplementary Fig. S3). With shoot-applied GA_4 the GPS1 ratio of the maturation zone increased in the in the stele + pericycle + endodermis and not the cortex and epidermis (Fig. 6, C, I, and J). This increase only in the tissue enclosed by the Casparian strip would be consistent with GA being transported from shoot to root, through the vascular tissue. In the elongation zone, where the Casparian strip is not yet developed (Barberon 2017), and the phloem unloads into the root tissue (Ross-Elliott et al. 2017), we observed an increase in GPS1 ratio across all layers of tissue (Fig. 6, D, K, and L). This is in accordance with the observed shoot-root transport of fluorescent GA_3 and GA_4 (Shani et al. 2013).

Summarizing, we show that WL + FR treatment of seedling shoots leads to increased GA levels in the lateral root primordia and the main root elongation zone, and that GA_4 application reduces lateral root density and lateral root zone length similar to WL + FR. Finally, we confirm that shoot-applied GA is likely transported to the root, which indicates that GA could play an important role in transducing the WL + FR signal from the shoot to the root. Next, we investigated the downstream regulation following GA_4 application and how this integrates with the regulation of lateral root growth by WL + FR.

DELLAs confer the GA effects on the root in WL + FR

In order to understand how GA is involved in the regulation of lateral root development by WL + FR we started with the knockout mutant of the 5 *della* GA repressor proteins, which should have very little response to GA_4 application since GA responses typically occur via GA-dependent DELLA protein degradation (Schwechheimer 2012). Compared to the *Ler* background, the *della pentuple* mutant had an increased hypocotyl length in WL and WL + FR (Supplementary Fig. S4A, consistent with a previous study Hayes et al. 2019), but did not respond further to GA application, as expected (Supplementary Fig. S4, A and D). *Ler* showed a reduction in lateral root density in WL + FR and in accordance with Col-0 this reduction was no longer present in the 10^2 nM GA_4 treatment (Supplementary Fig. S4, B and D). Importantly, the lateral root density and lateral root zone length of the *della pentuple* mutant was not affected by WL + FR, or GA_4 treatment (Supplementary Fig. S4, B to D). We previously showed that the lateral root primordium Stages 5 and 6 are enriched in WL + FR, consistent with a reduced lateral root emergence (van Gelderen et al. 2018, 2021) and this phenotype was also lost in the *della pentuple* mutant (Supplementary Fig. S4E). Since DELLAs are degraded upon binding of GA to its receptor GID1 (Schwechheimer 2012), we tested whether our 10^2 nM GA_4 treatment effectively degraded DELLAs in the root. Protein levels of the DELLA protein RGA fused to GFP, visualized through confocal microscopy, were clearly visible in mock treatment, and disappeared after 3 d of 10^2 nM GA_4 (Supplementary Fig. S5A), confirming that this GA_4 treatment was sufficient to degrade one of the major DELLAs. We subsequently used an anti-RGA antibody to observe the RGA response to WL + FR. In accordance with our expectations and data, WL + FR led to a decrease in RGA in the shoot and importantly also the root (Supplementary Fig. S5, B and D) and as expected, 10^3 nM 24 h PAC treatment stabilized RGA (Supplementary Fig. S5C). These results show that the DELLAs are important for the root response to shoot-exposed WL + FR and that they confer the effect of GA on the root system in WL + FR.

Interactions between GA and HY5 regulate root responses to WL + FR

A previously established regulator of the root developmental response to WL + FR is the HY5 transcription factor (van Gelderen et al. 2018). We, therefore, investigated if the HY5 and GA pathways jointly regulate root development in response to light, using the *hy5 hyh* (*hy5 homolog*) double mutant. WL + FR and GA_4 application both increased the hypocotyl length of Col-0 as well as *hy5 hyh* double mutant (Fig. 7A). The interactive effects of WL + FR and GA_4 application on root development observed in Col-0 were absent in the *hy5 hyh* mutant (Fig. 7, C and D). Since GA4 effects are particularly strong at high concentrations, we also performed an experiment with 10^4 nM GA_4, instead of 10^2 nM. The strongly increased inhibition of main root length, reduction of lateral root density, lateral root zone length and the increase in root hairs found in Col-0 (Fig. 7, H to K), were partially absent in *hy5 hyh,* indicating a substantially reduced sensitivity of this mutant's root response to GA_4 application. *hy5 hyh* lateral root density was decreased by 10^4 nM GA_4, however, this was mainly due to the extra main root length, as the lateral root zone length strikingly did not change (Fig. 7 I, J, and L). Overall, the roots of *hy5 hyh* seedlings looked very similar in 10^4 nM GA_4 compared to 0 nM GA_4 (Fig. 7L), in stark contrast to Col-0, which had almost no laterals left, and many, very long root hairs (Fig. 7, K and L, see arrowhead). We used the

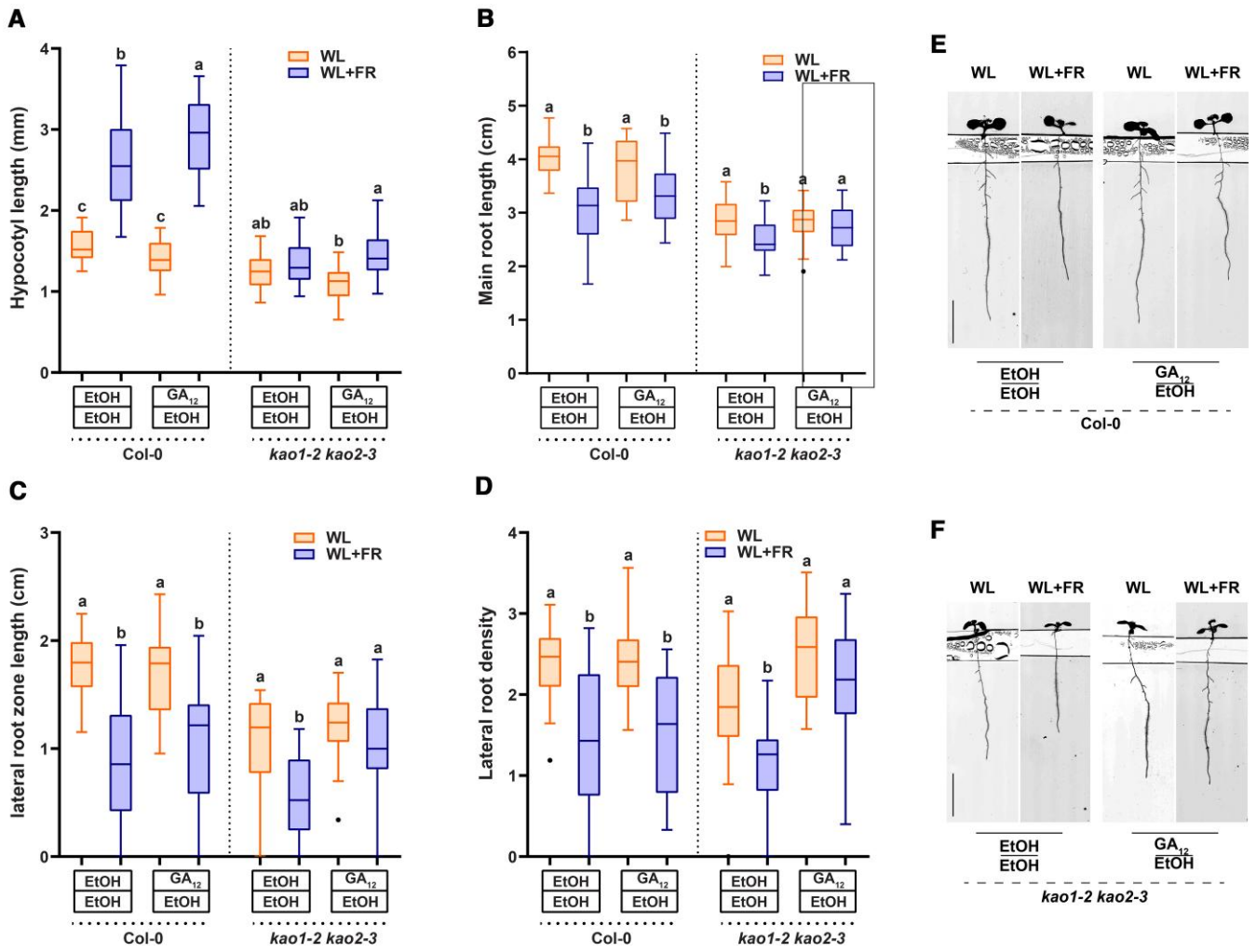

Figure 5. GA_{12} application on the shoot has a negligible effect on Col-0 root growth, but does affect the *kao1-2 kao2-3* mutant. Nine-d-old Col-0 and *kao1-2 kao2-3* seedlings, treated with either a mock solution or with 20 nM GA_{12} on the shoot, grown in WL or WL + FR. **A** to **D)** Hypocotyl length, main root length, lateral root zone length and lateral root density, respectively. **E** and **F)** Representative seedlings scanned at Day 9, the horizontal lines in the images are the borders between the agar layers and the "trench" between them. (All graphs) Means were statistically significant based on a 2-way ANOVA; letters denote significant difference between treatments based on a post hoc Tukey test ($P < 0.05$, $n \geq 20 \leq 30$); whiskers show the distribution.

RGA antibody to see if this lack of GA sensitivity in *hy5 hyh* would be visible at the protein level. The decrease in RGA detected in WL + FR in Col-0 was stronger than the decrease in the *hy5 hyh* double mutant (Supplementary Fig. S5, D and E), confirming that the *hy5 hyh* mutant is indeed less sensitive to GA.

Next, we also investigated the reverse interaction: effects of GA_4 application on HY5 abundance, using a *hy5-2 pHY5:HY5-GFP* line. We treated seedlings for 2 d with 10^2 nM GA_4 and EtOH mock control, after which they were analyzed by western blot and by confocal microscopy. A western blot did not show significant differences between treatments (Supplementary Fig. S6). However, using confocal microscopy we were able to see that across all lateral root primordia stages there was a significant increase in HY5-GFP abundance in response to GA_4 application (Fig. 8, A and B). Conversely, inhibiting endogenous GA levels with PAC did not significantly affect HY5-GFP abundance (Fig. 8, C and D). HY5-GFP in the main root meristem did not have a significant increase due to GA_4 treatment (Fig. 8, G, H, and K). We then treated seedlings with GA_4 on the shoot and analyzed HY5-GFP in the shoot, lateral root primordia and main root meristem. GA_4 shoot treatment caused an increase of HY5-GFP in the lateral root primordia similar to whole-plate GA_4 treatment (Fig. 8, B, E, and F), with no change of HY5-GFP in the main root meristem (Fig. 8, I to K). Therefore, the data seems to point to a specific upregulation of HY5 in the lateral root primordia, also explaining why no significant difference was observed on western blot of whole roots. Interestingly, HY5-GFP in the shoot apical meristem was decreased by GA_4 application (Fig. 8, L to N). This striking difference between shoot and root HY5-GFP responses to GA_4 application is consistent with the opposite effects of GA_4 on growth in the 2 different tissues: GA_4-induced reduction of HY5 will promote hypocotyl elongation, since HY5 represses hypocotyl growth in shade (Sellaro et al. 2011; Ortiz-Alcaide et al. 2019) (Fig. 4C), while the GA_4-induced promotion of HY5-GFP in the root will lead to a shorter, reduced root system (van Gelderen et al. 2018) (Fig. 4D).

HY5 can repress auxin signaling related to lateral root development (Cluis et al. 2004; van Gelderen et al. 2018), and GA can post-translationally upregulate auxin transporters (Willige et al. 2011; Mäkilä et al. 2023). Therefore, we used the C3PO auxin sensor cassette (Küpers et al. 2023) to estimate auxin abundance and auxin signaling response. In the lateral root primordia of Stages 1 to 4,

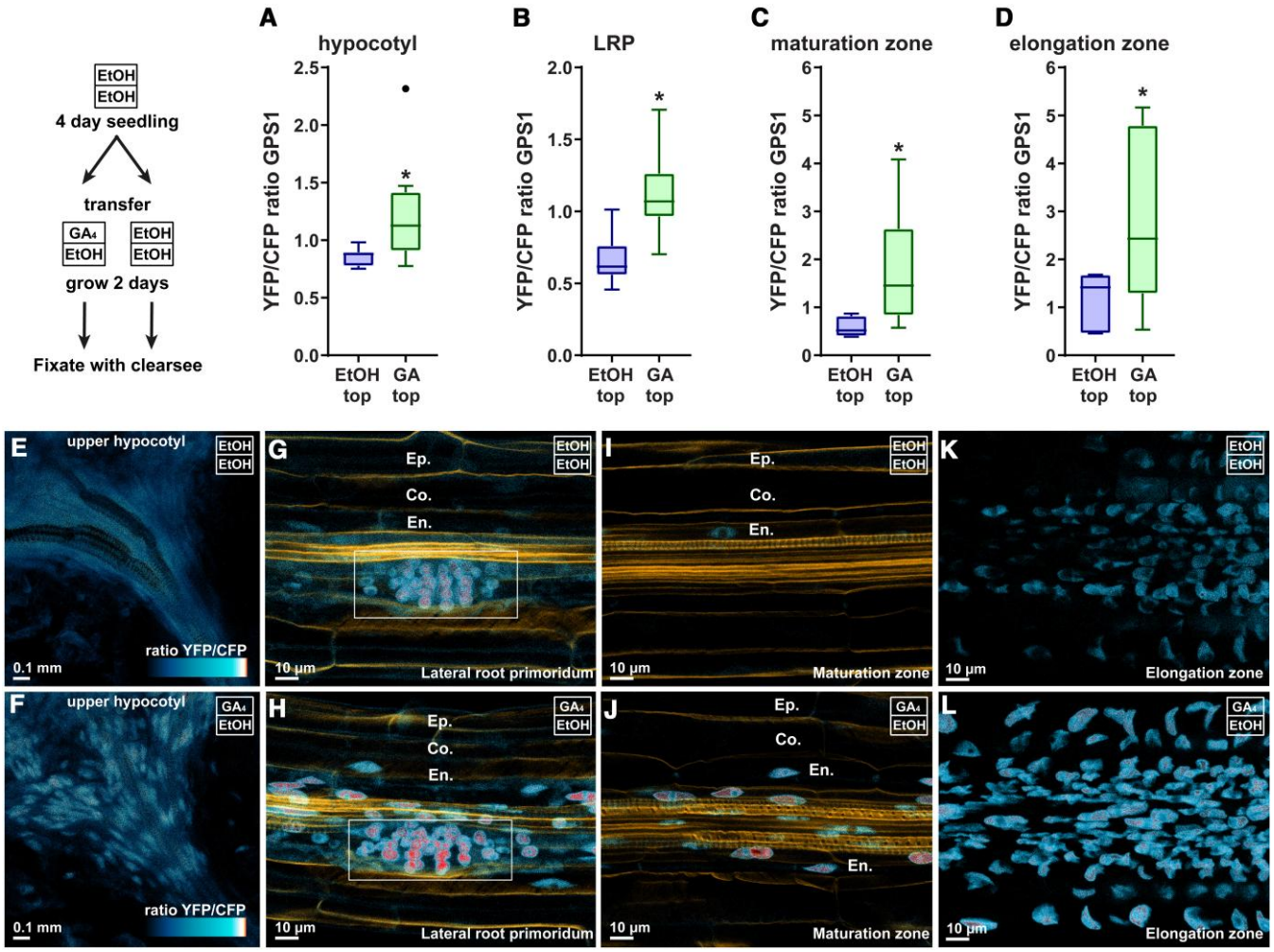

Figure 6. Shoot application of GA_4 leads to strictly defined GPS1 FRET changes in the root. Confocal microscopy experiment with quantifications **A** to **D)** and representative images **E** to **L)**. GPS1 seedlings were handled in the same manner as depicted in Fig. 4A, with the difference being that the seedlings were fixed with ClearSee after 2 d. GPS1 line was either treated for 2 d with shoot GA_4, or with mock EtOH. **A** to **D**) GPS1 YFP/CFP ratios of the hypocotyl **A)**, lateral root primordia Stages 2 to 6 **B)**, maturation zone **C)**, elongation zone **D)**. **E to I)** Representative images used for calculating **B)**: **E** and **F)**, **C)**: **G** and **H)**, **D)**: **I** and **J)**. White box emphasizes the LRP, and the epidermis (Ep.), cortex (Co.), and endodermis (En.) layers have been highlighted in **G** to **I)** and a cell-wall stain with directred23 is visible in orange. Scale bars = 10 μm. *significant difference based on student's *t*-test ($P < 0.05$, $n \geq 9$); whiskers show the distribution.

both auxin abundance and response, as measured by the R2D2 and DR5v2 parts of the sensor respectively, were promoted by shoot-GA treatment (Supplementary Fig. S7, A to C). In the phloem unloading zone, auxin levels increased due to shoot GA (Supplementary Fig. S7, D and E), while in the main root meristem, auxin signaling was reduced by shoot-GA treatment (Supplementary Fig. S7, F and G). Overall, GA_4-shoot treatment led to an increase in auxin and HY5 abundance, and though these data show that GA can crosstalk with auxin signaling, they also highlight the complexity of interactions between GA_4, HY5 and auxin and future studies are needed to resolve if and how auxin regulation by GA and HY5 either or not is functionally associated with root responses to shoot-exposed FR light.

HY5 and shoot-GA_4 repress auxin signaling and lateral root development-related genes

To obtain insight into the downstream transcriptional effects of shoot-GA_4 treatment and the role of HY5 in this process we performed a qPCR analysis on shoot and root samples of seedlings treated with shoot-GA_4 or control ethanol (1:10000) in either wild type or *hy5 hyh* mutant background. We tested genes known to be downstream of or associated with HY5 (*NRT2;1*, *BBX21*; Datta et al. 2007; Chen et al. 2016; Xu et al. 2016; van Gelderen et al. 2021), GA biosynthesis and signaling genes (*GA3ox1*, *GA2ox6*, *GA2ox8* [Hedden and Thomas 2012], and RGA), auxin transport and signaling genes (*PIN3*, *LAX3*, *ARF19*, *SHY2*, *IAA2*; Li et al. 2015; Vilches-Barro and Maizel 2015), genes involved in lateral root emergence (*IDA*, *HAE*; Kumpf et al. 2013), and *PIF3*.

HY5 and *HYH* itself were transcriptionally affected by GA_4: *HYH* was downregulated in the shoot (Supplementary Fig. S8A), while *HY5* was downregulated in the root (Fig. 9A). HY5-GFP protein levels did not change in whole-root samples (Supplementary Fig. S6). This discrepancy between gene expression and protein response, may be related to different periods of GA exposure and the strong post-translational regulation of HY5 via COP1 (Lau and Deng 2012). We were mainly interested in the effects of shoot-GA on gene expression in the root of wild type and the *hy5 hyh* mutant. Two genes, *GA3ox1* and *NRT2;1*, responded with a similar pattern of expression throughout the treatments; both showed reduced

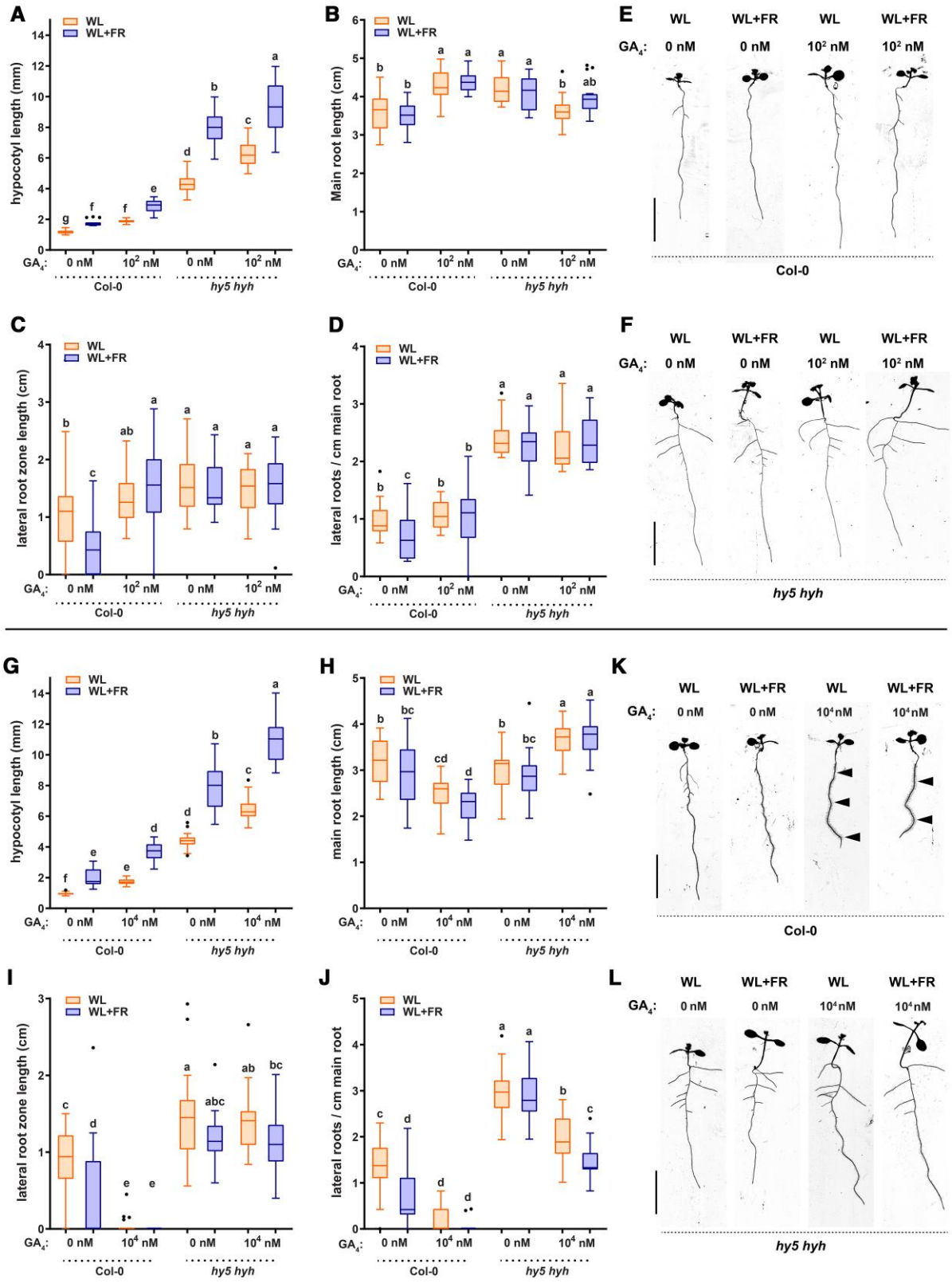

Figure 7. The *hy5 hyh* mutant has no lateral root development reduction in WL + FR nor in GA_4 treatment and responds less severely to a very high dose of GA_4. Seedlings of Col-0 and *hy5 hyh* were grown for 9 d according to the schedule on Supplementary Fig. S1A. Scans of 9-d-old seedlings treated with EtOH 1:10,000 in the medium or 10^2 nM GA_4 and analyzed on **A)** hypocotyl length; **B)** main root length; **C)** lateral root density; **D)** lateral root zone length. **E** and **F)** Representative seedling images of the experiment in **A** to **D)**, the arrowheads in **K)** point to excess root hairs in the 10^4 nM GA_4 treatment. **G** to **L)** Similar setup as in **A** to **F)**, but then with 10^4 nM GA_4. scale bar = 1 cm. Means were statistically significant based on a 2-way ANOVA; letters denote significant difference between treatments based on a post hoc Tukey test ($P < 0.05$, $n \geq 15$); whiskers show the distribution.

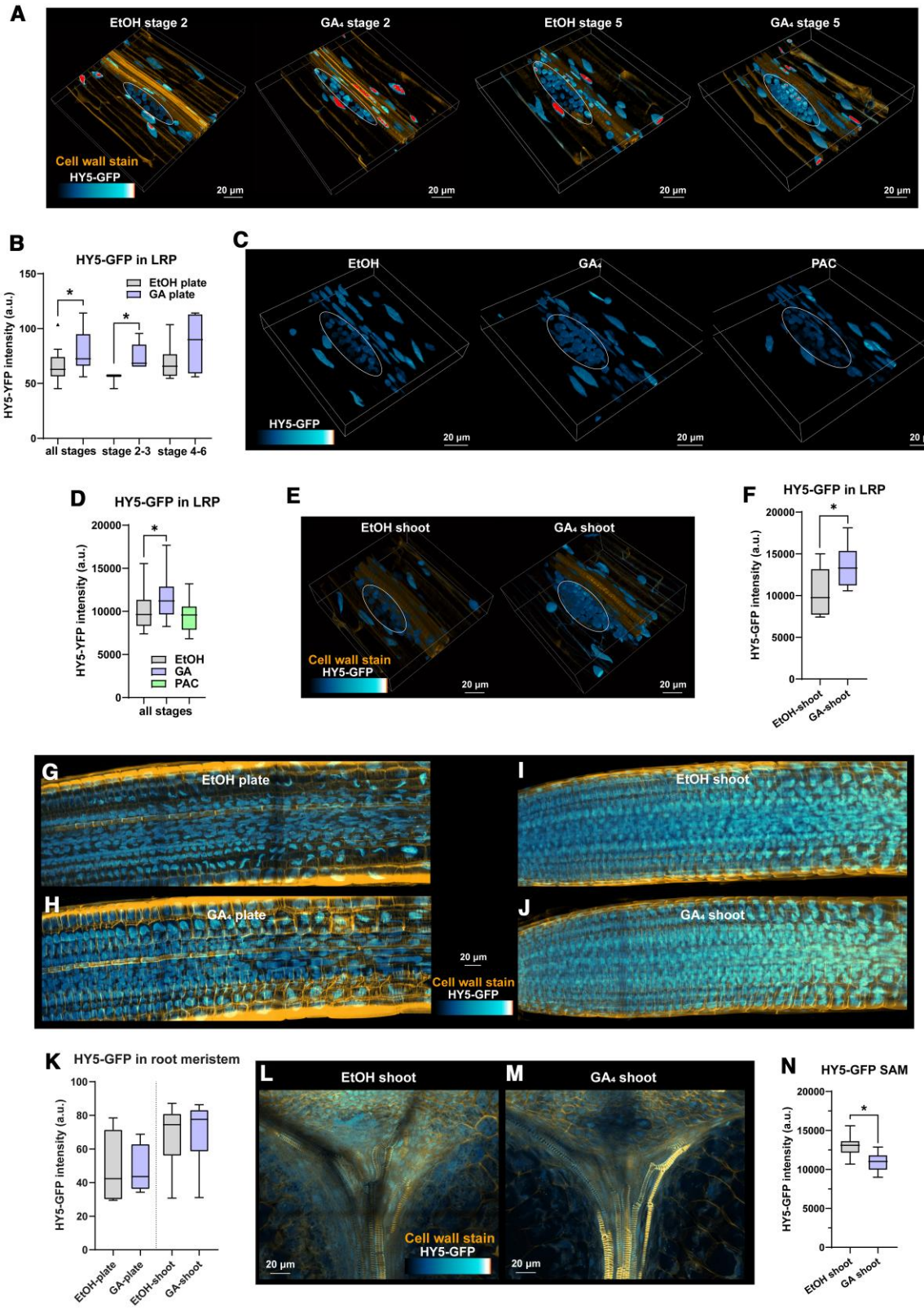

Figure 8. GA application leads to an increase in HY5-GFP in the lateral root primordia. Confocal images and quantifications of 6-d-old *hy5-2 pHY5:HY5-GFP* seedlings treated with mock or GA_4 on the whole plate for 2 d **A** to **D**; **G, H, and K)**, or on the shoot for 2 d, similar to Figs. 4 to 6 **E** and **F** to **N)**. **A, C,** and **E)** 3D projections of representative images of lateral root primordia treated with EtOH (mock) or GA_4. **B, D,** and **F)** Quantifications of lateral root Stages 2 to 6 accompanying **A, C,** and **E)**, respectively. **G to J)** Maximum intensity projections of representative images of main root meristems treated with EtOH (mock) or GA_4, with accompanying quantification **K)**. (The scale bar applies to all 4 images.) **L** and **M)** Maximum intensity projections of representative images of the shoot apical meristem region treated with EtOH (mock) or GA_4, and with quantification **N)**. All images show HY5-GFP in blue-to-white-to-red lookup table and a direct red23 cell wall staining in orange. *significant difference based on student's *t*-test **F** and **H)** and 1-way ANOVA **B**, **D)** ($P < 0.05$, $n = \geq 10 \leq 20$); whiskers show the distribution.

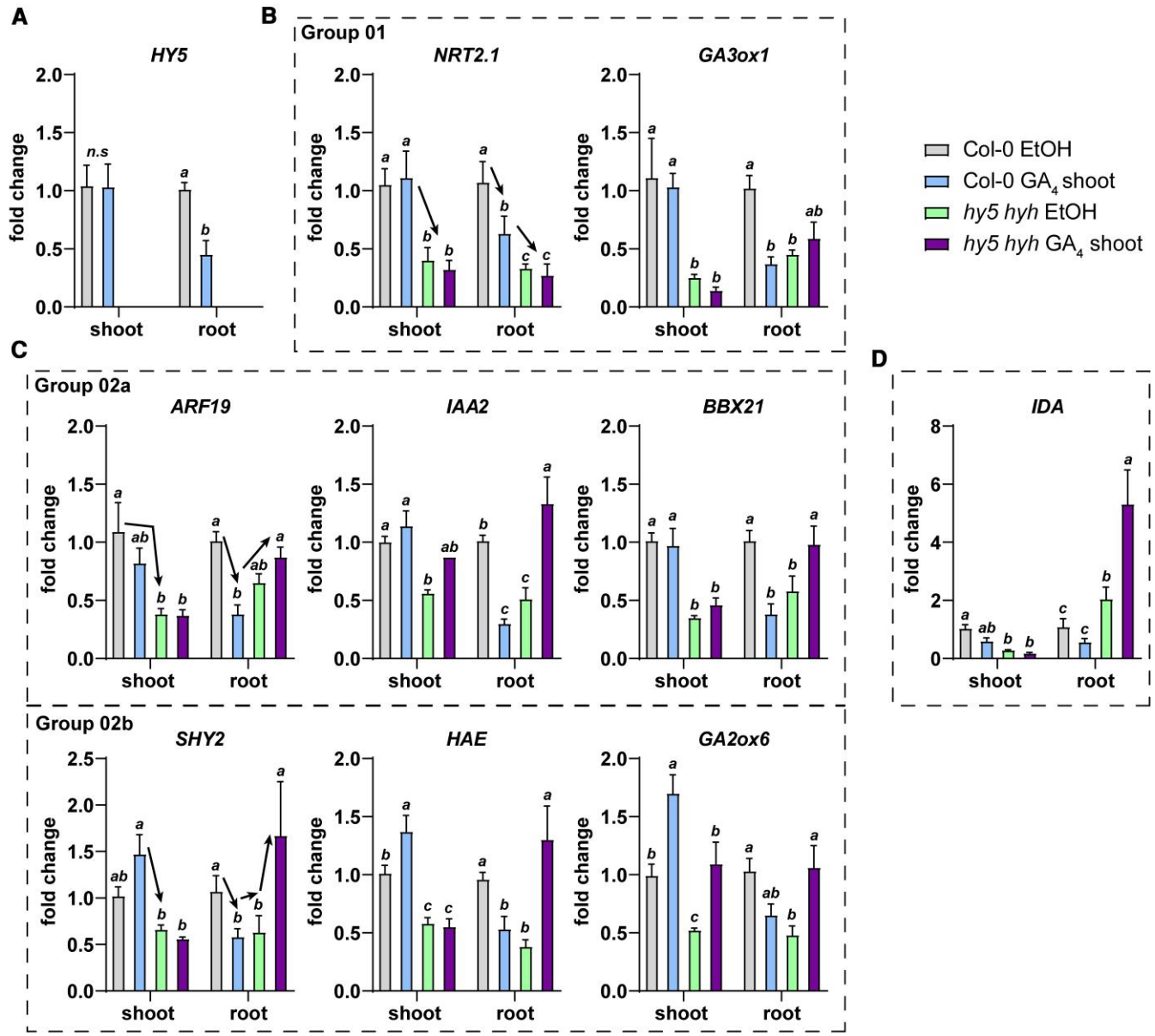

Figure 9. qPCR analysis shows repressive effect of GA_4-shoot treatment on target gene expression in root, which is modulated by *hy5 hyh* mutation. RT-qPCR analysis of shoot and root samples of 5-d-old seedlings (Col-0 and *hy5 hyh*), transferred to mock or GA_4-shoot 24 h before harvesting. **A)** *HY5* expression values (not detectable in *hy5 hyh* mutant). **B)** Group 01 genes, **C)** Group 02a and 02b genes, **D)** *IDA* expression values. Arrows show the changes in expression associated with that particular Group of genes. Expression values were analyzed according to the $\Delta\Delta^{CT}$ method and normalized against the Col-0 mock sample for both shoot and root respectively. Statistical significance was determined by 2-way ANOVA with a Newman–Keuls post hoc test ($P > 0.05$, $n = 4$); error bars show the SEM.

expression in *hy5 hyh* compared to Col-0, and were downregulated by GA_4 shoot treatment in the root tissues only of Col-0 seedlings, but not in those of *hy5 hyh* (Fig. 9B). As shown previously, the nitrate transporter gene *NRT2.1* is regulated via *HY5* and is involved in the root WL + FR response (van Gelderen et al. 2021), while GA3ox1 is important in the later steps of GA biosynthesis (Hedden and Thomas 2012).

A second, larger group had a similar response in the GA-shoot treatment, where this caused a downregulation in the root, but in the *hy5 hyh* mutant roots these genes were then upregulated by GA (Fig. 9C, Supplementary Fig. S8B, Group 2a). This group seemed to be regulated by GA, but in this case the GA response in the root was modified by the *hy5 hyh* mutant, but not completely dependent on it. Four of these genes, (*SHY2, HAE, GA2ox6, GA2ox8*) were upregulated by GA in the shoot, while the rest (*ARF19, BBX21, IAA2, RGA*), were not (Fig. 9C, Supplementary Fig. S8B, Group 2b). One gene, *IDA* (involved in lateral root emergence), was regulated particularly strongly via *HY5 HYH* since it was downregulated by GA in both shoot and root of Col-0, but its expression was enhanced in the *hy5 hyh* mutant and increased further in the GA-shoot treatment (Fig. 9D). Finally, a third group contained *PIF3* and *LAX3*, where the expression changes were relatively minor and not statistically significant (Supplementary Fig. S8C). Overall, shoot GA_4 treatment mainly had a repressive effect on the expression of the tested genes in the root. In most cases, the *hy5 hyh* mutation also resulted in a reduction in expression, meaning that in those cases HY5 would normally promote expression. However, in the *hy5 hyh* mutant the GA_4-shoot effect was often opposite of that in wild

type or was lost, indicating that *HY5* gates the GA response and highlighting the crosstalk between HY5 and GA.

To obtain more evidence for the role of HY5 in the downstream transcriptional response and at the same time the local effect of GA_4, we performed an experiment with a *HY5* inducible line, driven by an estradiol-inducible cassette (Siligato et al. 2016), coupled to a lateral root primordium specific promoter (*pGATA23*) (De Rybel et al. 2010). This line was made in a wild type background to simulate the effect of a strong HY5 increase. We induced expression of *pGATA23-XVE:HY5-YFP* by estradiol treatment and added a paclobutrazol treatment in the same agarose solution in order to assess the effects of HY5 without endogenous GA levels affecting it. Tested genes were reduced in expression by HY5 induction (Fig. 10, B, D, E, G, and H; Supplementary Fig. S9), with the exception of *GATA22, NRT2.2*, and *GA3ox1* (Supplementary Fig. S9). Interestingly, the PAC treatment did modulate some of the effects of the HY5 induction. *LAX3, SHY2, GA2ox6*, and *RGA* were further repressed (Fig. 10, D, E, and G), while *GATA22* was further increased (Supplementary Fig. S9) when endogenous GA production was inhibited. In a similar experiment, but with the addition of a WL + FR treatment, we performed a ChIP-qPCR analysis to quantify the binding of HY5-YFP to the promoters of the genes tested for qPCR in Fig. 10 that also contained high affinity HY5 binding sites (Song et al. 2008). Since we used an inducible HY5-YFP line, we had 3 negative controls: the "mock" DMSO treatment (compared to estradiol), a general anti-igg antibody (compared to anti GFP/YFP) and a promoter without a HY5 binding site. The beta estradiol induction of HY5 led to binding of HY5-YFP to the promoters of *HY5* itself (Fig. 10C). *HY5-YFP* induction led to binding of HY5 to the promoters of *NRT2.1* (Fig. 10C), *LAX3* and *SHY2* (Fig. 10F), and *GA2ox6* and *HAE* (Fig. 10I). A strong increase of HY5 expression coincided with a repression in expression of these genes (Fig. 10, A, B, D, E, G, and H). Interestingly, WL + FR led to an increase in HY5-YFP binding for all genes concerned (Fig. 10, C, F, and I). For some genes PAC treatment led to a clear decrease in promoter binding of HY5-YFP (*GA2ox6, HAE* Fig. 10I), while for others PAC led to a small decrease (*HY5, NRT2.1, LAX3* and *SHY2* Fig. 10, C and F). Thus, the specific HY5-YFP induction at the lateral root primordium development and initiation sites led to binding of HY5-YFP to the promoters of key genes for lateral root development and also to the promoter of a GA modifying enzyme. This was accompanied by a reduction in expression of these genes. PAC treatment had a mild effect on HY5 promoter binding and expression effects, while WL + FR treatment led to an increase in promoter binding. In many of the same genes, shoot-GA_4 treatment led to a repression in expression, in accordance with the positive effect of GA on HY5 protein amounts, while the effect of shoot-GA_4 effect on gene expression was reversed in the *hy5 hyh* mutant.

Discussion

We have shown previously that above-ground competitive responses can lead to a reduction in root growth, by a reduction in lateral root emergence regulated through HY5 (van Gelderen et al. 2018) and that this response depends upon the nutrient status of the plant (van Gelderen et al. 2021). Importantly, in these studies only the shoot is in an environment with a low R:FR ratio, since the roots are shielded from the light via a cover around the plate and barrier in the plate (van Gelderen et al. 2018). Now we show that these responses are modulated via Gibberellin. Whole-plate GA application has shown that lower GA_4 levels modulate the root response to FR light application on the shoot (WL + FR) and that higher GA_4 levels inhibit root growth. When GA biosynthesis is inhibited, via PAC application, we observed a reduction in root growth and a loss of the WL + FR phenotype. The reason that both GA_4 addition and the block of GA biosynthesis can give similar phenotypes at certain concentrations, may lie in the fact that root growth can be repressed by ectopic expression of DELLAs (Heo et al. 2011; Zhang et al. 2011), mimicking PAC application, but that normal DELLA signaling is also necessary to allow root growth (Ubeda-Tomás et al. 2008, 2009), which is important when applying physiologically relevant levels of GA. With the use of the GPS1 GA-FRET sensor (Rizza et al. 2017, 2021), we were able to show that GA is increased in the lateral root primordia and in the elongation zone of the root. Shoot-application of GA_4 and the GA-biosynthesis inhibitor uniconazole has previously been shown to reduce root growth (Bidadi et al. 2010). In the shoot, gibberellin biosynthesis is upregulated and GA accumulate in low R:FR (Djakovic-Petrovic et al. 2007; Kohnen et al. 2016).

Gibberellins are essential regulators in hypocotyl growth (Rizza et al. 2017) and cooperate with auxin in the low R:FR response of adult plant petioles (Küpers et al. 2023). GA_3 and GA_4 can be transported from shoot to root through the phloem (Shani et al. 2013). In our experiments, we have shown that shoot application of GA_4 leads to a reduction in root growth, but more importantly, also to a loss of the WL + FR effect. Shoot-applied GA_4 led to a clear response of the GPS1 sensor in the root: in the vasculature, lateral root primordium, and the elongation zone, which is consistent with mobility of GA_4 from shoot to root. GA_{12} can also be transported from shoot to root (Regnault et al. 2015), and was able to affect the lateral root density of the *kao1-2 kao2-3* double mutant, but not in wild type. We do not know how much of the GA_{12} that we applied to the shoot, will have reached the root in these experiments, nor do we know how much of that GA_{12} will have been converted to bioactive GA. The study of these precursor GA forms is rather challenging, since the purification of these forms is difficult and unspecific. Therefore, we were limited in the amount of GA_{12} that we could apply. If this technical hurdle could be cleared, then future studies could address this issue. Ideally these would be complemented with grafting studies using dedicated mutant/wild-type combinations, but grafting of young Arabidopsis seedlings is technically challenging to the level that it does not really allow for detailed quantitative physiology. Even so, our data together strongly indicate that shoot-root transport of GA plays an important role in the root response to WL + FR. The question is then how shoot-derived GA_4 affects the development of the root. Gibberellin signaling acts through the proteasomal degradation of the DELLA transcriptional regulators. The *della pentuple* mutant did not have a WL + FR root phenotype, and did not respond to GA application, thus supporting the notion that the GA_4 response is mediated by DELLAs. DELLAs frequently act by directly binding to transcription factors whose activity is then inhibited (Davière and Achard 2016) and they can affect main root growth through the interaction of RGA with SCARECROW-LIKE3 (Heo et al. 2011; Zhang et al. 2011). GA_3 (thus presumably GA_4 as well) can enhance the responsiveness of the root to IAA (Li et al. 2015). In our experiments, GA_4-shoot treatment also led to a decrease in detected auxin (R2D2), auxin signaling (dr5v2) and a repression of auxin-related gene expression (qPCR). GA can also promote auxin signaling by relieving DELLA repression of ARF6 and ARF8 (Oh et al. 2014), and to understand the effects of GA on root auxin response gene expression, future studies could investigate if DELLAs also interact with ARFs that are more involved in

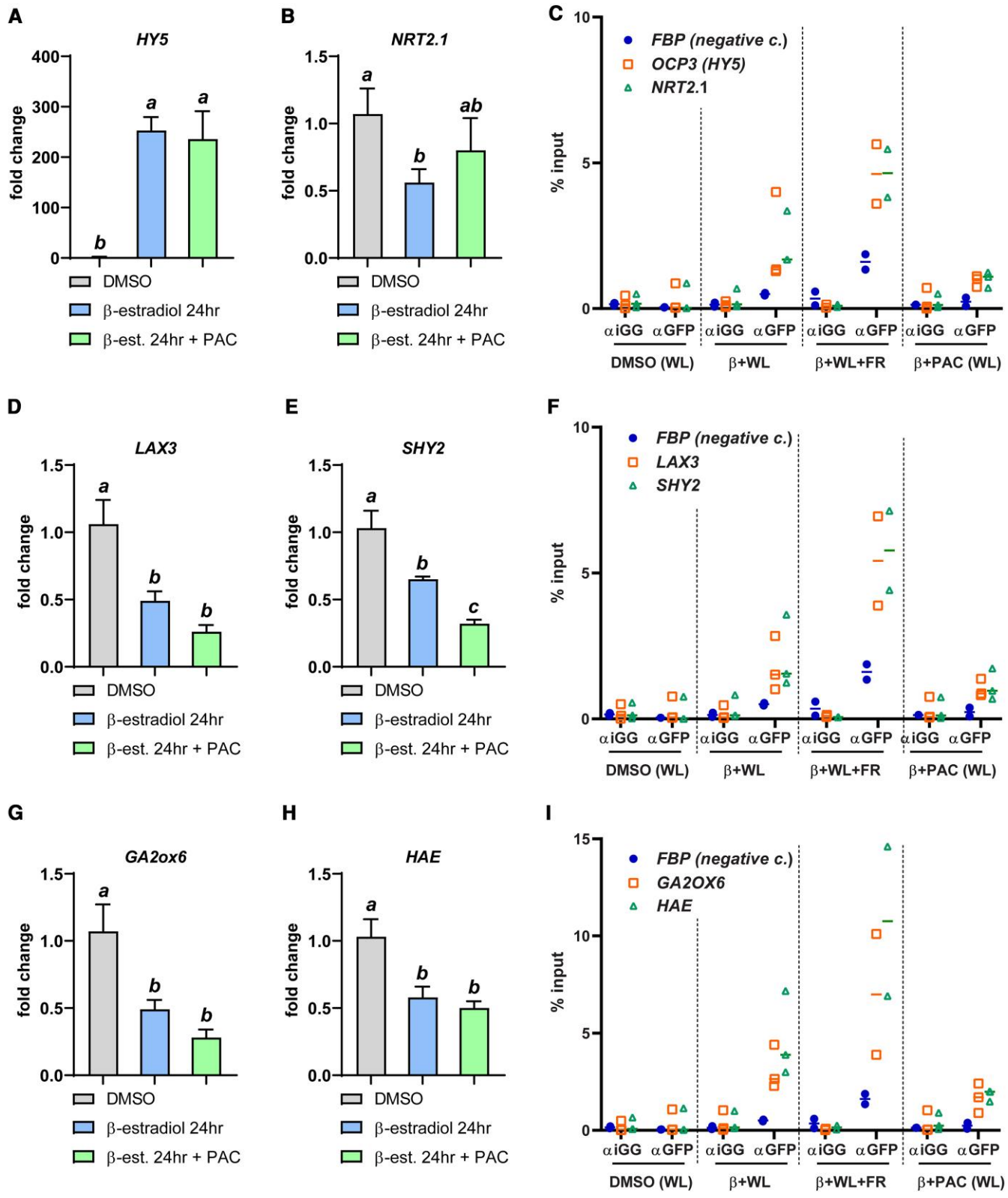

Figure 10. A qPCR and ChIP-qPCR approach shows repressive effect of HY5 on expression of lateral root development and GA-related genes. **A, B, D, E, G,** and **H)** RT-qPCR analysis of root samples of 5-d-old seedlings (Col-0 *pGATA23-XVE:HIS-HY5-YFP*), induced on the root by beta-estradiol, mock induced and treated with PAC 24 h before harvesting. Expression values were analyzed according to the $\Delta\Delta^{CT}$ method and normalized against the Col-0 mock sample for both shoot and root respectively. Statistical significance was determined by 1-way ANOVA with a Newman–Keuls post hoc test ($P > 0.05$, $n = 4$); error bars show the SEM. **C, F,** and **I)** Chromatin Immuno Precipitation (ChIP)—RT-qPCR experiment on the same Col-0 *pGATA23-XVE:HIS-HY5-YFP* line, with 5-d-old seedlings, treated 24 h earlier with mock, beta-estradiol with additional WL + FR or PAC treatment. Roots were sampled and the isolated and sheared chromatin was incubated with either a control anti-iGG antibody, or an anti-GFP antibody, probing for HY5-YFP. RT-qPCR values were calculated to a percentage of the input-DNA before immunoprecipitation. Horizontal bars show the mean value of the data.

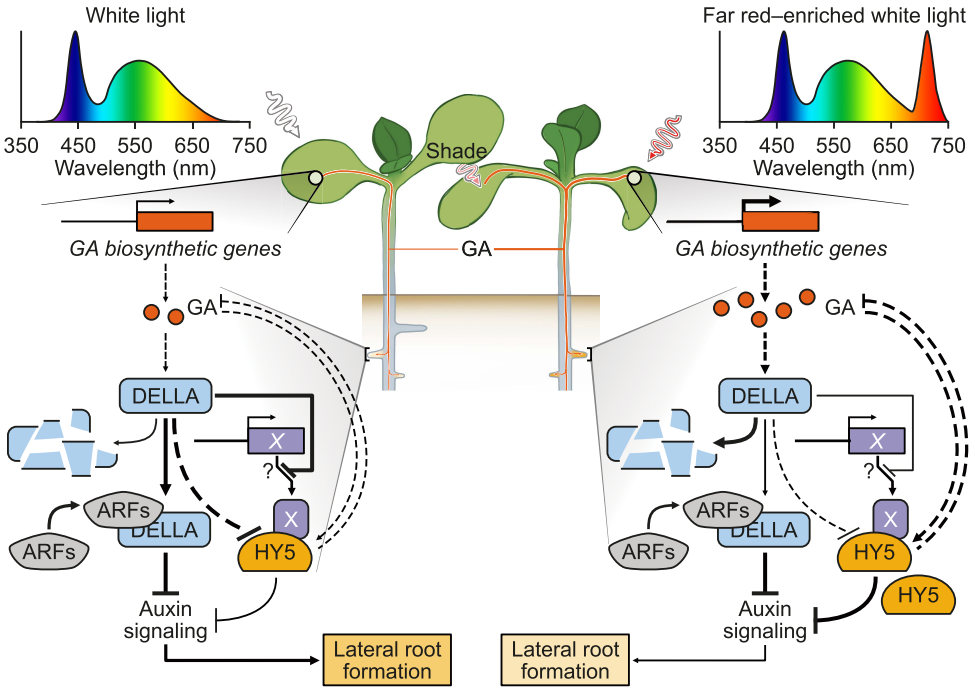

Figure 11. The role of Gibberellins (GA_4) and HY5 in modulating lateral root growth during above-ground plant-plant competition. The proximity of neighboring plants leads to a relative increase in the amount of FR light, simulated in our experiments with the addition of FR light to the growth light (WL + FR). This leads to an increase in GA, which can travel through the phloem toward the root tissues. There, GA leads to DELLA degradation, which indirectly leads to an increase in HY5, possibly via the de-repression of HY5 cofactors or an as-of-yet unidentified mechanism. Alternatively, DELLA could repress auxin signaling directly by binding to ARF transcription factors. HY5 can repress auxin signaling and thus a brake on lateral and main root development. However, HY5 can also repress GA biosynthesis. Solid arrows mean a direct effect, while dashed arrows indicate an indirect effect.

the regulation of root auxin levels and root development, such as ARF7 and ARF19.

The *hy5 hyh* double mutant, which showed no root response to WL + FR treatment, was also less responsive to GA_4 treatment, suggesting that GA_4 response in roots involves HY5. GA_4-shoot treatment led to an increase of HY5 in the lateral root primordia and HY5 is known to be able to repress auxin signaling in the root and lateral root emergence (Cluis et al. 2004; Sibout et al. 2006; van Gelderen et al. 2018), which was confirmed by the qPCR and ChIP-qPCR data after *HY5* induction. Furthermore, the qPCR results showed that in the *hy5 hyh* mutant, the effect of GA_4 application was modified: In *hy5 hyh* roots, GA_4-shoot treatment led to an increase in auxin-related expression, indicating that HY5 normally represses this GA response. Together these results paint a picture whereby low R:FR detected by the shoot, leads to increased gibberellin transport to the root, either or not in parallel with putative HY5 translocation. In the root. gibberellin stimulates HY5, which leads to repression of auxin signaling and thus of (lateral) root growth (Fig. 11). An open question is then how gibberellin leads to a stimulation of HY5 protein levels. Until now, there has been no evidence that RGA or any other DELLA interacts with HY5. RGA can bind to and inhibit PIF3 and BZR1, key regulators of light and hormone signaling (De Lucas et al. 2008; Bai et al. 2012; Gallego-Bartolome et al. 2012) which could be interesting collaborative factors for HY5 action, since PIF3 and BZR1 can interact with HY5 and act as a cofactor of HY5 (Chen et al. 2013; Li and He 2016). Future studies could investigate the interactions that occur between HY5 and other transcriptional regulators in the root, to really pinpoint the mechanism of regulation.

In this study we have mostly used the Col-0 ecotype, to have consistency in root phenotypes. However, certain mutants are only available in *Ler* background, which has a different root system architecture compared to Col-0. However, this root system still responds to WL + FR, although in a slightly differently manner then Col-0 (Supplementary Fig. S4C). In the future it could be interesting to see how different ecotypes of Arabidopsis compare in the response to above ground supplemental FR.

Materials and methods

Plant material and growth conditions

Arabidopsis thaliana plants were grown in a controlled environment growth chamber with a 16-h-light/8-h-dark cycle, temperature of 20 °C and a light level of PAR ~140 $\mu mol/m^2/s$. Knockout lines used were: *hy5 hyh* (Zhang et al. 2017), *dellap pentuple (gai-t6 rga-t2 rgl1-1 rgl2-1 rgl3-4)*, *pif1 pif3 and pif1 pif3 pif4 pif5 pif7* (Leivar et al. 2020), *ga1-3* (Michaels and Amasino 1999). The *kao1-2* (salk_136249C), and *kao2-3* (salk_135819) alleles were crossed to create the *kao1-2 kao2-3* double mutant. Fluorescent marker lines and sensors used were: *NLS-GPS1* and *NLS-GPS1-NR* (Rizza et al. 2017), *hy5-2 pHY5:HY5-GFP* (Zhang et al. 2017), *pRGA:GFP-RGA* (Silverstone et al. 2001). *C3PO* (Küpers et al. 2023). Col-0 *pGATA23-XVE:HIS-HY5-YFP* was created by stably transforming Col-0 with a tissue specific vector system (Siligato et al. 2016), harboring a newly cloned *HY5* coding sequence (see molecular cloning).

Square plate growth and root phenotyping

For root phenotyping seeds were surface sterilized using a 1 h treatment with chlorine gas. Seeds were sown on ½ MS 0.1% MES, pH 5.8, 0.8% plant agar plates, at 25 per plate (12.5 × 12.5 × 1.75 cm) by scattering them on a plate and then the plates were put in the dark at 4 °C for 6 d for seed stratification. Plates were put in the growth chamber (16/8 light/dark photoperiod, PAR = 140 $\mu mol\ m^{-2}\ s^{-1}$, 21 °C) shortly after subjective dawn and allowed to germinate for 24 h. Then the germinated seeds were

transferred on a new plate, containing either the treatment chemical or a mock treatment, 25 seeds on a line, at 9 cm height. Just below the seeds the D-root (Silva-Navas et al. 2015) insert was placed and the root part of the plate was covered by a black cover (see van Gelderen et al. 2018). Plates were then returned to the growth chamber after which either white light treatment continued or the WL + FR treatment started. For the WL + FR treatment plates were placed 20 cm in front of a row of FR LEDs (Phillips GreenPower LED research module far red, 24Vdc/10W) to achieve a R:FR ratio of 0.1 in the shoot part, which was measured inside the plate using a small, flexible R:FR light meter (Skye Spectrosense2). After 4 d of growth, seedlings were transferred in the afternoon to a new plate (5 to 6 seedlings per plate) to ensure homogeneous growth and prevent intermingling of root systems. For the compartmentalized plates of Fig. 4, a PVC plastic piece was glued into a standard 12 cm Greiner plate using epoxy resin 2-component glue. Agar layers were poured separately in the respective compartments, and during transfer, seedlings were carefully arranged so that only the shoot part was touching the top agar layer and only the root part the bottom agar layer (Supplementary Fig. S2B). For the experiments in Fig. 5 seedlings were transferred not on Day 4, but Day 6. A trench was cut in the agar using sterile surgical blades and seedlings were carefully arranged so that they traversed the trench (Supplementary Fig. S2F). The *kao1-2 kao2-3* mutant was stratified and germinated in 25 μM GA_3, before sowing on a normal ½ MS plate. GA_{12} was applied in a droplet of 0.1% agarose 20 nM GA_{12}. For all root phenotyping experiments, square Petri dishes were scanned at 600 or 1200 dpi using an EPSON V850 photonegative scanner. Experiments were analyzed using Smartroot (Lobet et al. 2011). The scans were converted from a color image to an 8bit grayscale image and contrast was enhanced to provide a better input for Smartroot. Hypocotyl length was analyzed either manually with a precision caliper after scanning, or by analyzing the scanned images with ImageJ.

DIC microscopy and lateral root primordia analysis

Seedlings used for lateral root primordia analysis were fixed and cleared according to a previously published protocol (Malamy and Benfey 1997). The seedlings were mounted in 50% glycerol and analyzed using a Zeiss Axioskop2 DIC microscope (40× Plan-NEOFLUAR DIC objective) with a Lumenera Infinity 1 camera.

Confocal microscopy and analysis

For confocal microscopy seeds were sown at 16 per plate and were transferred at Day 4 to GA_4 or PAC containing medium. Seedlings were fixed with 4% paraformaldehyde and cleared and stained according to a modified ClearSee protocol (Ursache et al. 2018). Confocal microscopy was performed with either a Zeiss Observer Z1 LSM7 confocal imaging system, with 405, 488, 514 and 563 nm excitation lasers, and fixed bandpass filters for CFP (450 to 480), YFP (530 to 560), and RFP (600LP), or a Zeiss LSM 880 Airyscan system using 453, 488, 514, and 563 lasers with electronically adjustable bandpass filters: CFP (460 to 490), YFP (525 to 560), and RFP (575 to 650). Laser and gain settings were set at the same level within experiments, to achieve optimal signal/noise ratio. Confocal z-stack images were made using a 40× NA1.2 oil immersion objective (both microscopes). Within experiments, pinhole, detector gain, laser power, and detector offset were the same. All images were analyzed using ICY http://icy.bioimageanalysis.org/), using the HK-means plugin to select individual nucleus regions.

RNA extraction and RT-qPCR expression analysis

For gene expression analyses, plants were sown at 16 seeds in a row and grown in the conditions mentioned above for 5 d. Between 15 to 19 seedlings were harvested per sample (from 2 plates) and only root tissues were used for RNA extraction. Four biological replicates were taken per treatment/genotype condition. The Qiagen plant RNeasy kit was used for RNA extraction. First-strand cDNA was made using the Thermo Scientific RevertAid H Minus Reverse Transcriptase, RiboLock RNase inhibitor, and Invitrogen random hexamer primers. RNA input into the cDNA reaction was kept equal within experiments, preferably at 1000 ng. Primers were designed preferably across introns and for 100- to 150-bp fragments with an annealing temperature of 60 °C with primer3plus (http://www.bioinformatics.nl/cgi-bin/primer3plus/primer3plus.cgi). Primers were tested for efficiency using generic Col-0 cDNA at a concentration range of 2.5 → 40 ng of cDNA per 5 mL reaction. qPCR reagents used were Bio-Rad SYBR-Green Mastermix on 384-well plates in a Life Technologies ViiA7 real-time PCR system. All CT values were normalized against 2 validated housekeeping genes: *ADENINE PHOSPHORIBOSYL TRANSFERASE1 and PROTEIN PHOSPHATASE 2A SUBUNIT A3*. The $\Delta\Delta^{CT}$ method was used to calculate relative expression values (Livak and Schmittgen 2001). Primer sequences are provided in Supplementary Table S1.

Chromatin immunoprecipitation

For the chromatin immuno precipitation (ChIP) experiment we used a modified version of a histone modification ChIP-seq protocol (Antunez-Sanchez et al. 2020; Ramirez-Prado et al. 2021). We used ~150 to 200 seedling roots per sample, and performed the chromatin isolation in 2 ml Eppendorf tubes, rather than falcon tubes. Shearing was done with a Diagenode Bioruptor, for a 20 to 30 min length of 30 s bursts, followed by 30 s of rest. The immunoprecipitation was performed in PCR strips, using Pierce protein A/G magnetic beads, Roche anti-GFP monoclonal antibody and Roche rabbit anti-igg antibody as control. Isolated DNA fragments were measured with a qBit DNA analyzer. For the RT-qPCR reactions, 20 to 50 pg of DNA was used per reaction, with the same reagents as described above.

Molecular cloning and plant transformation

We made a transgenic, estradiol-inducible, tissue-specific HY5 line (Col-0 *pGATA23-XVE:HIS-HY5-YFP*). We cloned the *pGATA23* promoter into an empty multisite gateway-compatible entry vector (p1R4-pGATA-XVE), by first PCR-amplifying a *pGATA23* fragment and with BshTI and XhoI restriction sites on the 5′ ends of the primers. We ligated this fragment into a pJet1.2 cloning vector. From this vector we excised and ligated the *pGATA23* fragment into p1R4-ML-XVE (Siligato et al. 2016). We created a pDONR207-HIS-HY5 entry vector by PCR amplifying from cDNA a HY5 fragment with flanking gateway sites and performing a BP reaction. We then performed a multisite gateway reaction using the entry vector with the p1R4-pGATA-XVE, pDONR207-HIS-HY5 and p2R3 YFP 3AT entry vectors in a pGII R3R4 entry vector (Siligato et al. 2016) (Addgene). Primers are shown in the Supplementary Table S1. This entry vector was then transformed to dh5a *E.coli*, and subsequently prepped and transformed into *AGL1 psoup A. tumefaciens*. The transformation of Arabidopsis flowering plants was done via a published floral dip method (Davis et al. 2009). Transformed T1 seeds were selected with hygromycin and propagated. ~20 T2 lines were selected based on Mendelian segregation to select for single inserts and also tested with epifluorescence microscopy for leaky expression and fast

and correct induction. ~5 T3 lines were selected for homozygosity with hygromycin and again tested for proper, fast non-leaky induction.

Western blotting

For western blots, seeds were grown on ½ MS media on square plates as discussed above. Seedling roots and shoots were separated via scalpel, cutting them on the plate followed by immediately freezing in liquid nitrogen. After homogenizing with a Retsch mixer-mill, 2× Laemli buffer (4% SDS, 120 mM Tris-HCl pH 6.8, 10% glycerol, 0.05% bromophenol blue, 5% beta-mercaptoethanol, 0.5× Roche protease inhibitor solution (from tablet)), was immediately added and samples were heated at 95 °C for 5 min. Samples were then spun down 1 min at 14,000 rpm on a tabletop centrifuge and the supernatant was loaded on SDS-PAGE gel according to standard SDS PAGE methods. Standard running gel buffer (1% SDS, 0,25 M Tris-glycine, pH 8,6) was used. A wet transfer method at 4 °C was employed using a transfer buffer of 25 mM Trizma base, 24 mM Glycine and 0.5% SDS in 40% ethanol. Blocking was done with 5% milk powder in TBS, overnight at 4 °C. After blocking primary and secondary antibodies were incubated 1 h at room temperature in TBS with 0.5% milk powder. Washing steps (4×) were done with TBS 0.1% tween buffers. Antibodies used were Roche anti GFP from mouse IgG1κ (clones 7.1 and 13.1), anti RGA (Agrisera Anti-RGA; product no: AS11 1630), Agrisera Goat anti-Rabbit IgG HRP conjugated (Product no: AS09 602) and Rabbit anti-Mouse IgG HRP conjugated (Product no: AS09 627). For blot developing, AgriseraECL SuperBright (Product no: AS16 ECL-S-100) was used. For loading control staining either a Coomassie stain or TGX protein stain were employed.

Data processing and statistics

For root system analysis Smartroot was employed (see phenotyping), and for confocal anaylsis we used Icy bioimage analysis (see Confocal microscopy and analysis). Data from Smartroot and Icy was processed and analyzed with R with a custom-made script. Two-way ANOVA testing with post hoc tests was done with R. Two-way ANOVA was used to query for significantly different means in genotype, treatment, and genotype–treatment interactions. If the 2-way ANOVA showed significant differences, a post hoc Newman–Keuls tests were performed to discover significant differences between pairs of means. Graphs were made using Graphpad Prism. For experiments with only a genotype or only a treatment difference, 1-way ANOVA and students' *t*-test were employed, which were calculated using Graphpad Prism. Boxplot graphs show min/max values excluding outliers, with outliers identified by a Tukey test as individual data points. Figures were composed using Adobe Illustrator.

Accession numbers

The gene accession numbers linking the genes studied in this paper with sequence information accessible on NCBI or TAIR can be found in Supplementary Table S2.

Acknowledgments

We thank Wouter Kohlen for donating GA_{12} for the experiment in Fig. 5, and Richard Paalman and Roxanne Lock for experimental optimizations. We thank Leonardo Jo for help with setting up ChIP-qPCR experiments and the Utrecht Scientific Instrument Workshop for their assistance with manufacturing custom plates. We thank Alexander Jones for sharing GPS1 lines and guidance on GPS1 imaging, Lanlan Zheng for sharing a collection of *HY5* lines. Finally, we would like to thank Patrick Achard and his group for producing and sharing the *kao1-2 kao2-3* mutant.

Author contributions

K.v.G. and R.P. designed the experiments and wrote the manuscript. K.v.G., K.v.d.V., C.-k.K., J.H., O.P., A.K., and P.P. performed and analyzed the experiments. T.A. performed experiments and provided technical assistance.

Supplementary data

The following materials are available in the online version of this article.

Supplementary Figure S1. Gibberellins are involved in FR-shoot-induced changes in root development.

Supplementary Figure S2. Compartmentalized plates have minimal diffusion after 7 d of vertical orientation and seedlings are carefully positioned across the border.

Supplementary Figure S3. GPS1 ratios in the outer root layers (cortex, epidermis) increase strongly with a whole plate GA4 treatment.

Supplementary Figure S4. The *della pentuple* mutant has no lateral root development reduction in WL + FR and does not respond to a GA4 treatment.

Supplementary Figure S5. WL + FR regulates RGA stability in the root and shoot and is gated by the hy5 hyh mutations.

Supplementary Figure S6. Western blot on HY5-GFP root samples shows no significant difference.

Supplementary Figure S7. GA4 shoot treatment leads to changes in auxin levels and signaling in root tissues.

Supplementary Figure S8. qPCR experiment with shoot GA4 treatment and hy5 hyh mutant, supplementary to Fig. 8.

Supplementary Figure S9. Additional qPCR data to Fig. 9.

Supplementary Table S1. Primers used in this study.

Supplementary Table S2. Gene accession numbers.

Funding

This research was funded by the Netherlands Organisation for Scientific Research (NWO), open competition grant 823.01.013 and Vici grant 865.17.002 to R.P. C.K. was funded by a scholarship of government sponsorship for overseas study, Taiwan, admission number 0991167-2-UK-004. K.v.G. is currently funded by the Emmy Noether program of the Deutsche Forschungsgemeinschaft (DFG) #GE 3355/1-1.

Conflict of interest statement. None declared.

Data availability

The data underlying this article will be shared on reasonable request to the corresponding author(s).

References

Antunez-Sanchez J, Naish M, Ramirez-Prado JS, Ohno S, Huang Y, Dawson A, Opassathian K, Manza-Mianza D, Ariel F, Raynaud C, et al. A new role for histone demethylases in the maintenance of plant genome integrity. *eLife*. 2020:9:e58533. https://doi.org/10.7554/eLife.58533

Bai M-Y, Shang J-X, Oh E, Fan M, Bai Y, Zentella R, Sun T, Wang Z-Y. Brassinosteroid, gibberellin and phytochrome impinge on a common transcription module in *Arabidopsis*. *Nat Cell Biol*. 2012:14(8):810–817. https://doi.org/10.1038/ncb2546

Ballaré CL, Pierik R. The shade-avoidance syndrome: multiple signals and ecological consequences. *Plant Cell Environ*. 2017:40(11):2530–2543. https://doi.org/10.1111/pce.12914

Barberon M. The endodermis as a checkpoint for nutrients. *New Phytol*. 2017:213(4):1604–1610. https://doi.org/10.1111/nph.14140

Barker R, Fernandez Garcia MN, Powers SJ, Vaughan S, Bennett MJ, Phillips AL, Thomas SG, Hedden P. Mapping sites of gibberellin biosynthesis in the *Arabidopsis* root tip. *New Phytol*. 2021:229(3):1521–1534. https://doi.org/10.1111/nph.16967

Bidadi H, Yamaguchi S, Asahina M, Satoh S. Effects of shoot-applied gibberellin/gibberellin-biosynthesis inhibitors on root growth and expression of gibberellin biosynthesis genes in *Arabidopsis thaliana*. *Plant Root*. 2010:4:4–11. https://doi.org/10.3117/plantroot.4.4

Binenbaum J, Weinstain R, Shani E. Gibberellin localization and transport in plants. *Trends Plant Sci*. 2018:23(5):410–421. https://doi.org/10.1016/j.tplants.2018.02.005

Bou-Torrent J, Galstyan A, Gallemí M, Cifuentes-Esquivel N, Molina-Contreras MJ, Salla-Martret M, Jikumaru Y, Yamaguchi S, Kamiya Y, Martínez-García JF, et al. Plant proximity perception dynamically modulates hormone levels and sensitivity in Arabidopsis. *J Exp Bot*. 2014:65(11):2937–2947. https://doi.org/10.1093/jxb/eru083

Chen D, Xu G, Tang W, Jing Y, Ji Q, Fei Z, Lin R. Antagonistic basic Helix-loop-Helix/bZIP transcription factors form transcriptional modules that integrate light and reactive oxygen Species signaling in *Arabidopsis*. *Plant Cell*. 2013:25(5):1657–1673. https://doi.org/10.1105/tpc.112.104869

Chen X, Yao Q, Gao X, Jiang C, Harberd NP, Fu X. Shoot-to-root mobile transcription factor HY5 coordinates plant carbon and nitrogen acquisition. *Curr Biol*. 2016:26(5):640–646. https://doi.org/10.1016/j.cub.2015.12.066

Cluis CP, Mouchel CF, Hardtke CS. The *Arabidopsis* transcription factor HY5 integrates light and hormone signaling pathways. *Plant J*. 2004:38(2):332–347. https://doi.org/10.1111/j.1365-313X.2004.02052.x

Crocco CD, Locascio A, Escudero CM, Alabadí D, Blázquez MA, Botto JF. The transcriptional regulator BBX24 impairs DELLA activity to promote shade avoidance in *Arabidopsis thaliana*. *Nat Commun*. 2015:6:1–32. https://doi.org/10.1038/ncomms7202

Datta S, Hettiarachchi C, Johansson H, Holm M. SALT TOLERANCE HOMOLOG2, a B-box protein in *Arabidopsis* that activates transcription and positively regulates light-mediated development. *Plant Cell*. 2007:19(10):3242–3255. https://doi.org/10.1105/tpc.107.054791

Davière JM, Achard P. A pivotal role of DELLAs in regulating multiple hormone signals. *Mol Plant*. 2016:9(1):10–20. https://doi.org/10.1016/j.molp.2015.09.011

Davis AM, Hall A, Millar AJ, Darrah C, Davis SJ. Protocol: streamlined sub-protocols for floral-dip transformation and selection of transformants in *Arabidopsis thaliana*. *Plant Methods*. 2009:5(1):3. https://doi.org/10.1186/1746-4811-5-3

De Lucas M, Davière JM, Rodríguez-Falcón M, Pontin M, Iglesias-Pedraz JM, Lorrain S, Fankhauser C, Blázquez MA, Titarenko E, Prat S. A molecular framework for light and gibberellin control of cell elongation. *Nature*. 2008:451(7177):480–484. https://doi.org/10.1038/nature06520

De Rybel B, Vassileva V, Parizot B, Demeulenaere M, Grunewald W, Audenaert D, Van Campenhout J, Overvoorde P, Jansen L, Vanneste S, et al. A novel aux/IAA28 signaling cascade activates GATA23-dependent specification of lateral root founder cell identity. *Curr Biol*. 2010:20(19):1697–1706. https://doi.org/10.1016/j.cub.2010.09.007

Djakovic-Petrovic T, Wit MD, Voesenek LACJ, Pierik R. DELLA protein function in growth responses to canopy signals. *Plant J*. 2007:51(1):117–126. https://doi.org/10.1111/j.1365-313X.2007.03122.x

Franklin KA, Whitelam GC. Phytochromes and shade-avoidance responses in plants. *Ann Bot*. 2005:96(2):169–175. https://doi.org/10.1093/aob/mci165

Gallego-Bartolome J, Minguet EG, Grau-Enguix F, Abbas M, Locascio a, Thomas SG, Alabadi D, Blazquez Ma. Molecular mechanism for the interaction between gibberellin and brassinosteroid signaling pathways in *Arabidopsis*. *Proc Natl Acad Sci U S A*. 2012:109(33):13446–13451. https://doi.org/10.1073/pnas.1119992109

Guo Z, Xu J, Wang Y, Hu C, Shi K, Zhou J, Xia X, Zhou Y, Foyer CH, Yu J. The phyB-dependent induction of HY5 promotes iron uptake by systemically activating FER expression. *EMBO Rep*. 2021:22(7):e51944. https://doi.org/10.15252/embr.202051944

Hayes S, Pantazopoulou CK, van Gelderen K, Reinen E, Tween AL, Sharma A, de Vries M, Prat S, Schuurink RC, Testerink C, et al. Soil salinity limits plant shade avoidance. *Curr Biol*. 2019:29(10):1669–1676.e4. https://doi.org/10.1016/j.cub.2019.03.042

Hedden P, Sponsel V. A century of gibberellin research. *J Plant Growth Regul*. 2015:34(4):740–760. https://doi.org/10.1007/s00344-015-9546-1

Hedden P, Thomas SG. Gibberellin biosynthesis and its regulation. *Biochem J*. 2012:444(1):11–25. https://doi.org/10.1042/BJ20120245

Heo J-O, Chang KS, Kim IA, Lee M-H, Lee SA, Song S-K, Lee MM, Lim J. Funneling of gibberellin signaling by the GRAS transcription regulator scarecrow-like 3 in the *Arabidopsis* root. *Proc Natl Acad Sci U S A*. 2011:108(5):2166–2171. https://doi.org/10.1073/pnas.1012215108

Hisamatsu T, King RW, Helliwell CA, Koshioka M. The involvement of gibberellin 20-oxidase genes in phytochrome-regulated petiole elongation of *Arabidopsis*. *Plant Physiol*. 2005:138(2):1106–1116. https://doi.org/10.1104/pp.104.059055

Inada S, Shimmen T. Regulation of elongation growth by gibberellin in root segments of Lemna minor. *Plant Cell Physiol*. 2000:41(8):932–939. https://doi.org/10.1093/pcp/pcd018

Kohnen MV, Schmid-Siegert E, Trevisan M, Petrolati LA, Sénéchal F, Müller-Moulé P, Maloof J, Xenarios I, Fankhauser C. Neighbor detection induces organ-specific transcriptomes, revealing patterns underlying hypocotyl-specific growth. *Plant Cell*. 2016:28(12):2889–2904. https://doi.org/10.1105/tpc.16.00463

Kumpf RP, Shi C-L, Larrieu A, Stø IM, Butenko MA, Peret B, Riiser ES, Bennett MJ, Aalen RB. Floral organ abscission peptide IDA and its HAE/HSL2 receptors control cell separation during lateral root emergence. *Proc Natl Acad Sci U S A*. 2013:110(13):5235–5240. https://doi.org/10.1073/pnas.1210835110

Küpers JJ, Snoek BL, Oskam L, Pantazopoulou CK, Matton SEA, Reinen E, Liao C-Y, Eggermont EDC, Weekamp H, Biddanda-Devaiah M, et al. Local light signaling at the leaf tip drives remote differential petiole growth through auxin-gibberellin dynamics. *Curr Biol*. 2023:33(1):75–85.e5. https://doi.org/10.1016/j.cub.2022.11.045

Küpers JJ, van Gelderen K, Pierik R. Location matters: canopy light responses over spatial scales. *Trends Plant Sci*. 2018:23(10):865–873. https://doi.org/10.1016/j.tplants.2018.06.011

Lau OS, Deng XW. The photomorphogenic repressors COP1 and DET1: 20 years later. *Trends Plant Sci*. 2012:17(10):584–593. https://doi.org/10.1016/j.tplants.2012.05.004

Leivar P, Martín G, Soy J, Dalton-Roesler J, Quail PH, Monte E. Phytochrome-imposed inhibition of PIF7 activity shapes photoperiodic growth in *Arabidopsis* together with PIF1, 3, 4 and 5.

Physiol Plant. 2020:169(3):452–466. https://doi.org/10.1111/ppl.13123

Li G, Zhu C, Gan L, Ng D, Xia K. GA3 enhances root responsiveness to exogenous IAA by modulating auxin transport and signalling in *Arabidopsis*. *Plant Cell Rep*. 2015:34(3):483–494. https://doi.org/10.1007/s00299-014-1728-y

Li Q-F, He J-X. BZR1 interacts with HY5 to mediate brassinosteroid- and light-regulated cotyledon opening in Arabidopsis in darkness. *Mol Plant*. 2016:9(1):113–125. https://doi.org/10.1016/j.molp.2015.08.014

Livak KJ, Schmittgen TD. Analysis of relative gene expression data using real-time quantitative PCR and the 2-ΔΔCT method. *Methods*. 2001:25(4):402–408. https://doi.org/10.1006/meth.2001.1262

Lobet G, Pagès L, Draye X. A novel image-analysis toolbox enabling quantitative analysis of root system architecture. *Plant Physiol*. 2011:157(1):29–39. https://doi.org/10.1104/pp.111.179895

Mäkilä R, Wybouw B, Smetana O, Vainio L, Solé-Gil A, Lyu M, Ye L, Wang X, Siligato R, Jenness MK, et al. Gibberellins promote polar auxin transport to regulate stem cell fate decisions in cambium. *Nat Plants*. 2023:9(4):631–644. https://doi.org/10.1038/s41477-023-01360-w

Malamy JE, Benfey PN. Organization and cell differentiation in lateral roots of *Arabidopsis thaliana*. *Development (Cambridge, England)*. 1997:124(1):33–44. https://doi.org/10.1242/dev.124.1.33

Michaels SD, Amasino RM. The gibberellic acid biosynthesis mutant ga1–3 of *Arabidopsis thaliana* is responsive to vernalization. *Dev Genet*. 1999:25(3):194–198. https://doi.org/10.1002/(SICI)1520-6408(1999)25:3<194::AID-DVG2>3.0.CO;2-2

Ni W, Xu S-L, Chalkley RJ, Pham TND, Guan S, Maltby DA, Burlingame AL, Wang Z-Y, Quail PH. Multisite light-induced phosphorylation of the transcription factor PIF3 is necessary for both its rapid degradation and concomitant negative feedback modulation of photoreceptor phyB levels in *Arabidopsis*. *Plant Cell*. 2013:25(7):2679–2698. https://doi.org/10.1105/tpc.113.112342

Oh E, Zhu JY, Bai MY, Arenhart RA, Sun Y, Wang ZY. Cell elongation is regulated through a central circuit of interacting transcription factors in the Arabidopsis hypocotyl. *eLife*. 2014:2014(3):1–19. https://doi.org/10.7554/eLife.03031

Ortiz-Alcaide M, Llamas E, Gomez-Cadenas A, Nagatani A, Martínez-García JF, Rodríguez-Concepción M. Chloroplasts modulate elongation responses to canopy shade by retrograde pathways involving HY5 and abscisic acid. *Plant Cell*. 2019:31(2):384–398. https://doi.org/10.1105/tpc.18.00617

Prasetyaningrum P, Mariotti L, Valeri MC, Novi G, Dhondt S, Inzé D, Perata P, van Veen H. Nocturnal gibberellin biosynthesis is carbon dependent and adjusts leaf expansion rates to variable conditions. *Plant Physiol*. 2020:185(1):228–239. https://doi.org/10.1093/plphys/kiaa019

Rademacher W. GROWTH RETARDANTS: effects on gibberellin biosynthesis and other metabolic pathways. *Annu Rev Plant Physiol Plant Mol Biol*. 2000:51:501–531. https://doi.org/10.1146/annurev.arplant.51.1.501

Ramirez-Prado J, Latrasse D, Benhamed M. Histone modification ChIP-seq on *Arabidopsis thaliana* plantlets. *Bio Protoc*. 2021:11(21). https://doi.org/10.21769/BioProtoc.4211

Reed JW, Foster KR, Morgan PW, Chory J. Phytochrome B affects responsiveness to gibberellins in *Arabidopsis*. *Plant Physiol*. 1996:112(1):337–342. https://doi.org/10.1104/pp.112.1.337

Regnault T, Davière J-M, Heintz D, Lange T, Achard P. The gibberellin biosynthetic genes AtKAO1 and AtKAO2 have overlapping roles throughout *Arabidopsis* development. *Plant J*. 2014:80(3):462–474. https://doi.org/10.1111/tpj.12648

Regnault T, Davière J-M, Wild M, Sakvarelidze-Achard L, Heintz D, Carrera Bergua E, Lopez Diaz I, Gong F, Hedden P, Achard P. The gibberellin precursor GA12 acts as a long-distance growth signal in Arabidopsis. *Nat Plants*. 2015:1(6):15073. https://doi.org/10.1038/nplants.2015.73

Rizza A, Tang B, Stanley CE, Grossmann G, Owen MR, Band LR, Jones AM. Differential biosynthesis and cellular permeability explain longitudinal gibberellin gradients in growing roots. *Proc Natl Acad Sci U S A*. 2021:118(8):e1921960118. https://doi.org/10.1073/pnas.1921960118

Rizza A, Walia A, Lanquar V, Frommer WB, Jones AM. In vivo gibberellin gradients visualized in rapidly elongating tissues. *Nat Plants*. 2017:3:803–813. https://doi.org/10.1038/s41477-017-0021-9

Ross-Elliott TJ, Jensen KH, Haaning KS, Wager BM, Knoblauch J, Howell AH, Mullendore DL, Monteith AG, Paultre D, Yan D, et al. Phloem unloading in arabidopsis roots is convective and regulated by the phloem pole pericycle. *eLife*. 2017:6:1–31. https://doi.org/10.7554/eLife.24125

Sakuraba Y, Kanno S, Mabuchi A, Monda K, Iba K, Yanagisawa S. A phytochrome-B-mediated regulatory mechanism of phosphorus acquisition. *Nat Plants*. 2018:4(12):1089–1101. https://doi.org/10.1038/s41477-018-0294-7

Schwechheimer C. Gibberellin signaling in plants—the extended version. *Front Plant Sci*. 2012:2:1–7. https://doi.org/10.3389/fpls.2011.00107

Sellaro R, Yanovsky MJ, Casal JJ. Repression of shade-avoidance reactions by sunfleck induction of HY5 expression in Arabidopsis: repression of shade-avoidance by sunflecks. *Plant J*. 2011:68(5):919–928. https://doi.org/10.1111/j.1365-313X.2011.04745.x

Shani E, Weinstain R, Zhang Y, Castillejo C, Kaiserli E, Chory J, Tsien RY, Estelle M. Gibberellins accumulate in the elongating endodermal cells of Arabidopsis root. *Proc Natl Acad Sci U S A*. 2013:110(12):4834–4839. https://doi.org/10.1073/pnas.1300436110

Shin A-Y, Han Y-J, Baek A, Ahn T, Kim SY, Nguyen TS, Son M, Lee KW, Shen Y, Song P-S, et al. Evidence that phytochrome functions as a protein kinase in plant light signalling. *Nat Commun*. 2016:7:11545. https://doi.org/10.1038/ncomms11545

Sibout R, Sukumar P, Hettiarachchi C, Holm M, Muday GK, Hardtke CS. Opposite root growth phenotypes of hy5 versus hy5 hyh mutants correlate with increased constitutive auxin signaling. *PLoS Genet*. 2006:2(11):e202. https://doi.org/10.1371/journal.pgen.0020202

Siligato R, Wang X, Yadav SR, Lehesranta S, Ma G, Ursache R, Sevilem I, Zhang J, Gorte M, Prasad K, et al. MultiSite gateway-compatible cell type-specific gene-inducible system for plants. *Plant Physiol*. 2016:170(2):627–641. https://doi.org/10.1104/pp.15.01246

Silva-Navas J, Moreno-Risueno MA, Manzano C, Pallero-Baena M, Navarro-Neila S, Tellez-Robledo B, Garcia-Mina JM, Baigorri R, Gallego FJ, Del Pozo JC. D-Root: a system for cultivating plants with the roots in darkness or under different light conditions. *Plant J*. 2015:84(1):244–255. https://doi.org/10.1111/tpj.12998

Silverstone AL, Jung H-S, Dill A, Kawaide H, Kamiya Y, Sun T. Repressing a repressor: gibberellin-induced rapid reduction of the RGA protein in *Arabidopsis*. *Plant Cell*. 2001:13(7):1555–1566. https://doi.org/10.1105/TPC.010047

Song YH, Yoo CM, Hong AP, Kim SH, Jeong HJ, Shin SY, Kim HJ, Yun D-J, Lim CO, Bahk JD, et al. DNA-binding study identifies C-box and hybrid C/G-box or C/A-box motifs as high-affinity binding sites for STF1 and LONG HYPOCOTYL5 proteins. *Plant Physiol*. 2008:146(4):1862–1877. https://doi.org/10.1104/pp.107.113217

Tal I, Zhang Y, Jørgensen ME, Pisanty O, Barbosa ICR, Zourelidou M, Regnault T, Crocoll C, Erik Olsen C, Weinstain R, et al. The *Arabidopsis* NPF3 protein is a GA transporter. *Nat Commun*. 2016:7:11486. https://doi.org/10.1038/ncomms11486

Tanimoto E. Interaction of gibberellin A3 and ancymidol in the growth and cell-wall extensibility of dwarf pea roots. *Plant Cell Physiol*. 1994:35(7):1019–1028. https://doi.org/10.1093/oxfordjournals.pcp.a078689

Ubeda-Tomás S, Federici F, Casimiro I, Beemster GTS, Bhalerao R, Swarup R, Doerner P, Haseloff J, Bennett MJ. Gibberellin signaling in the endodermis controls *Arabidopsis* root meristem size. *Curr Biol*. 2009:19(14):1194–1199. https://doi.org/10.1016/j.cub.2009.06.023

Ubeda-Tomás S, Swarup R, Coates J, Swarup K, Laplaze L, Beemster GTS, Hedden P, Bhalerao R, Bennett MJ. Root growth in *Arabidopsis* requires gibberellin/DELLA signalling in the endodermis. *Nat Cell Biol*. 2008:10(5):625–628. https://doi.org/10.1038/ncb1726

Ursache R, Andersen TG, Marhavý P, Geldner N. A protocol for combining fluorescent proteins with histological stains for diverse cell wall components. *Plant J*. 2018:93(2):399–412. https://doi.org/10.1111/tpj.13784

van Gelderen K, Kang C, Li P, Pierik R. Regulation of lateral root development by shoot-sensed far-red light via HY5 is nitrate-dependent and involves the NRT2.1 nitrate transporter. *Front Plant Sci*. 2021:12:660870. https://doi.org/10.3389/fpls.2021.660870

van Gelderen K, Kang C, Paalman R, Keuskamp D, Hayes S, Pierik R. Far-red light detection in the shoot regulates lateral root development through the HY5 transcription factor. *Plant Cell*. 2018:30(1):101–116. https://doi.org/10.1105/tpc.17.00771

Vilches-Barro A, Maizel A. Talking through walls: mechanisms of lateral root emergence in *Arabidopsis thaliana*. *Curr Opin Plant Biol*. 2015:23:31–38. https://doi.org/10.1016/j.pbi.2014.10.005

Willige BC, Isono E, Richter R, Zourelidou M, Schwechheimer C. Gibberellin regulates PIN-FORMED abundance and is required for auxin transport-dependent growth and development in *Arabidopsis thaliana*. *Plant Cell*. 2011:23(6):2184–2195. https://doi.org/10.1105/tpc.111.086355

Xu D, Jiang Y, Li J, Lin F, Holm M, Deng XW. BBX21, an *Arabidopsis* B-box protein, directly activates *HY5* and is targeted by COP1 for 26S proteasome-mediated degradation. *Proc Natl Acad Sci U S A*. 2016:113(27):7655–7660. https://doi.org/10.1073/pnas.1607687113

Yoshida H, Tanimoto E, Hirai T, Miyanoiri Y, Mitani R, Kawamura M, Takeda M, Takehara S, Hirano K, Kainosho M, et al. Evolution and diversification of the plant gibberellin receptor GID1. *Proc Natl Acad Sci U S A*. 2018:115(33):7844–7853. https://doi.org/10.1073/pnas.1806040115

Zhang Y, Li C, Zhang J, Wang J, Yang J, Lv Y, Yang N, Liu J, Wang X, Palfalvi G, et al. Dissection of HY5/HYH expression in *Arabidopsis* reveals a root-autonomous HY5-mediated photomorphogenic pathway. *PLoS One*. 2017:12(7):e0180449. https://doi.org/10.1371/journal.pone.0180449

Zhang Z-L, Ogawa M, Fleet CM, Zentella R, Hu J, Heo J-O, Lim J, Kamiya Y, Yamaguchi S, Sun T. SCARECROW-LIKE 3 promotes gibberellin signaling by antagonizing master growth repressor DELLA in Arabidopsis. *Proc Natl Acad Sci U S A*. 2011:108(5):2160–2165. https://doi.org/10.1073/pnas.1012232108